

1 ***Klebsiella pneumoniae* survives within macrophages by avoiding delivery to lysosomes.**

2 Catalina March^{1,2†}, Victoria Cano^{1,2†}, Nacho Aguiló^{2,3}, Enrique Llobet^{1,2}, David Moranta^{1,2},
3 Verónica Regueiro^{1,2}, Maria Isabel Millán-Lou^{2,3}, Carlos Martín^{2,3}, Junkal Garmendia^{2,4}, José A.
4 Bengoechea^{1,2,5,6}.

5 Laboratory Microbial Pathogenesis, Fundació d'Investigació Sanitària de les Illes Balears (FISIB),
6 Bunyola, Spain¹; Program Host-Pathogen interactions, Centro de Investigación Biomédica en Red
7 Enfermedades Respiratorias (CIBERES), Spain²; Grupo de Genética de Micobacterias, Dpto.
8 Microbiología, Medicina Preventiva y Salud Pública, Universidad de Zaragoza, Zaragoza, Spain³;
9 Instituto de Agrobiotecnología, CSIC-Universidad Pública de Navarra-Gobierno de Navarra,
10 Mutilva, Spain⁴; Consejo Superior de Investigaciones Científicas (CSIC), Madrid, Spain⁵, Centre
11 for Infection and Immunity, Queen's University Belfast, United Kingdom⁶

12 † These authors contributed equally to this work.

13
14 *Corresponding author:

15 Prof. José A. Bengoechea

16 Centre for Infection and Immunity,

17 Queen's University Belfast

18 Health Sciences Building,

19 97 Lisburn Rd. Belfast, UK BT9 7AE

20 Phone: +44 (0) 28 9097 2260; Fax: +44 (0) 28 9097 2671

21 E-mail: j.bengoechea@qub.ac.uk

22
23 Running title: *Klebsiella* intracellular survival

24

25 **SUMMARY**

26 *Klebsiella pneumoniae* is an important cause of community-acquired and nosocomial
27 pneumonia. Evidence indicates that *Klebsiella* might be able to persist intracellularly within a
28 vacuolar compartment. In this work, we demonstrate that *K. pneumoniae* survives killing by
29 macrophages by manipulating phagosome maturation. Engulfment of *K. pneumoniae* was
30 dependent on host cytoskeleton, cell plasma membrane lipid rafts and the activation of PI 3-
31 kinase (PI3K). Microscopy studies revealed that *K. pneumoniae* resides within a vacuolar
32 compartment, the *Klebsiella* containing vacuolae (KCV), which traffics within vacuoles
33 associated with the endocytic pathway. In contrast to UV-killed bacteria, alive bacteria did
34 not colocalize with markers of the lysosomal compartment. Our data suggest that *K.*
35 *pneumoniae* triggers a programmed cell death in macrophages displaying features of
36 apoptosis. Our efforts to identify the mechanism(s) whereby *K. pneumoniae* prevents the
37 fusion of the lysosomes to the KCV uncovered the central role of the PI3K-Akt-Rab14 axis to
38 control the phagosome maturation. We propose that agents targeting PI3K/Akt might provide
39 selective alternatives to manage *K. pneumoniae* pneumonias. We were keen to identify the
40 *Klebsiella* factors necessary for intracellular survival. Our data revealed that the capsule is
41 dispensable if bacteria were not opsonized. The environment found by *Klebsiella* within the
42 KCV triggered the downregulation of the expression of *cps*.

43

44 INTRODUCTION

45 In the late nineteenth century, Eli Metchnikoff appreciated phagocytosis as a key process in
46 the battle against pathogens. Phagocytosis can be conceptually divided into phagosome formation
47 and its subsequent evolution into a degradative compartment, a process termed phagosome
48 maturation. This is important because the nascent phagosome is not microbicidal. Maturation not
49 only aids clearing infection, but also generates and routes antigens for presentation on MHC
50 molecules in order to activate the adaptive immune system (Trombetta and Mellman. 2005).
51 Phagosome maturation involves the sequential acquisition of different proteins, many of them of the
52 endocytic pathway (Vieira *et al.* 2002, Flannagan *et al.* 2012). Thus, during and/or immediately after
53 phagosome closure, the phagosome fuses with early endosomes, acquiring Rab5 and early
54 endosome antigen 1 (EEA1). The phagosome rapidly loses the characteristics of early endosome
55 and acquires late endosome features. The late phagosome is positive for Rab7, the mannose-6-
56 phosphate receptor, lysobisphosphatidic acid, lysosome-associated membrane proteins (Lamps) and
57 CD63. Ultimately, the organelle fuses with lysosomes to form the phagolysosome, identified by the
58 presence of hydrolytic proteases, such as processed cathepsin D, cationic peptides and by an
59 extremely acidic luminal pH which is regulated primarily by the vacuolar (V-type) ATP-ase
60 complex. In the course of maturation, an oxidative system formed by the NADPH oxidase and
61 ancillary proteins is also activated.

62 Many pathogens have developed strategies to counteract the microbicidal action of
63 macrophages (Flannagan *et al.* 2009, Sarantis and Grinstein. 2012). Some pathogens inhibit
64 phagocytosis. For example, the role of capsule polysaccharides in preventing opsonophagocytosis
65 has been appreciated for many pathogens including *Neisseria meningitidis*, *Staphylococcus aureus*
66 and *streptococci*. Others, such as enteropathogenic *Escherichia coli*, inhibit engulfment by blocking
67 PI 3-kinase (PI3K) signaling whereas *Yersinia* species inhibits phagocytosis by injecting type III
68 secretion effectors. Conversely, *Salmonella typhimurium* induces its own uptake and, once inside a
69 modified phagosome, triggers macrophage death by a caspase-1 dependent process called pyroptosis

1
2 70 (Fink and Cookson. 2007). *Brucella* spp. resist an initial macrophage killing to replicate in a
3
4 71 compartment segregated from the endocytic pathway with endoplasmic reticulum properties (von
5
6 72 Bargen *et al.* 2012).

7
8 73 *Klebsiella pneumoniae* is a Gram negative capsulated pathogen which causes a wide range
9
10 74 of infections, from urinary tract infections to pneumonia, being particularly devastating among
11
12 75 immunocompromised patients with mortality rates between 25% and 60% (Sahly and Podschun.
13
14 76 1997). *K. pneumoniae* is an important cause of community-acquired pneumonia in individuals with
15
16 77 impaired pulmonary defences and is a major pathogen for nosocomial pneumonia. Pulmonary
17
18 78 infections are often characterized by a rapid clinical course thereby leaving very short time for an
19
20 79 effective antibiotic treatment. *K. pneumoniae* isolates are frequently resistant to multiple antibiotics
21
22 80 (Munoz-Price *et al.* 2013), which leads to a therapeutic dilemma. In turn, this stresses out the
23
24 81 importance of pulmonary innate defense systems to clear *K. pneumoniae* infections.
25
26
27

28 82 Resident alveolar macrophages play a critical role in the clearance of bacteria from the lung
29
30 83 by their capacity for phagocytosis and killing. It has been shown that depletion of alveolar
31
32 84 macrophages results in reduced killing of *K. pneumoniae in vivo* (Broug-Holub *et al.* 1997, Cheung
33
34 85 *et al.* 2000). This suggests that *Klebsiella* countermeasures against phagocytosis would be
35
36 86 important virulence factors. Supporting this notion, *K. pneumoniae* capsule (CPS) reduces
37
38 87 phagocytosis by neutrophils and macrophages (March *et al.* 2013, Cortes *et al.* 2002b, Rigueiro *et al.*
39
40 88 2006, Alvarez *et al.* 2000) and CPS mutant strains are avirulent not being able to cause pneumonia
41
42 89 and urinary tract infections (Cortes *et al.* 2002b, Lawlor *et al.* 2005, Camprubi *et al.* 1993).
43
44
45

46 90 *K. pneumoniae* has been largely considered as an extracellular pathogen. However, there are
47
48 91 reports showing that *K. pneumoniae* is internalized *in vitro* by different cell types being able to
49
50 92 persist intracellularly for at least 48 h (Oelschlaeger and Tall. 1997). It has been also reported the
51
52 93 presence of intracellular *Klebsiella* spp. within a vacuolar compartment inside human macrophages,
53
54 94 mouse alveolar macrophages and lung epithelial cells *in vivo* (Cortes *et al.* 2002b, Fevre *et al.*
55
56 95 2013, Willingham *et al.* 2009, Greco *et al.* 2012). This study was designed to investigate the
57
58
59
60

1
2 96 interaction between *K. pneumoniae* and macrophages. We report that *K. pneumoniae* survives
3
4 97 within macrophages by deviating from the canonical endocytic pathway and residing in a unique
5
6 98 intracellular compartment which does not fuse with lysosomes. Finally, we present evidence
7
8 99 indicating that *K. pneumoniae* has the potential to kill and escape from the phagocyte.
9

100

101

102 RESULTS

103 *K. pneumoniae* survives inside macrophages.

104 To explore whether *K. pneumoniae* resides inside macrophages *in vivo*, macrophages were
105 isolated from the bronchoalveolar lavage of mice infected intranasally with *K. pneumoniae* strain
106 43816 (hereafter Kp43816R). Microscopy analysis revealed the presence of intracellular bacteria in
107 10% of the recovered macrophages. Immunofluorescence experiments showed that 99 % \pm 7 of the
108 intracellular bacteria did not colocalize with the lysosomal marker cathepsin D (Fig 1A). Z-stack
109 projections confirmed that bacteria were located intracellularly (data not shown).

110 To assess the intracellular survival of *K. pneumoniae* in macrophages in more detail, we
111 standardized the infection conditions of the mouse macrophage cell line MH-S with *K. pneumoniae*
112 Kp43816R. We optimized the time of bacteria-cell contact (30, 60 and 120 min), the multiplicity of
113 infection (MOI) (100, 50 or 10 bacteria per cell), and the antibiotic treatment necessary to kill the
114 remaining extracellular bacteria after the contact. To synchronize infection, plates were centrifuged
115 at 200 x g during 5 min and intracellular bacteria were enumerated after macrophage lysis with
116 0.5% saponin in PBS. We found that 90 min treatment with a combination of gentamicin (300
117 μ g/ml) and polymyxin B (15 μ g/ml) was necessary to kill 99.9% of the extracellular bacteria. The
118 highest numbers of engulfed bacteria were obtained after 120 min of contact with a MOI of 100:1.
119 However, these conditions also triggered a significant decrease in cell viability as detected by the
120 trypan blue exclusion method. 30 min of contact and a MOI of 50:1 were the conditions in which
121 no decrease in cell viability was observed and, therefore, they were used in the subsequent
122 experiments.

1
2 123 To investigate the molecular mechanisms used by mouse macrophages to engulf Kp43816R,
3
4 124 infections were carried out in the presence of drugs which specifically inhibit host cell functions
5
6 125 (Fig 1B). Cytochalasin D and nocodazol reduced the engulfment of Kp43816R hence indicating that
7
8 126 Kp43816R phagocytosis requires the assembly of F-actin and the host microtubule network.
9
10 127 Methyl- β -cyclodextrin (M β CD), which depletes cholesterol from host cell membranes, was
11
12 128 employed to analyse the involvement of lipid rafts in Kp43816R phagocytosis. Cholesterol
13
14 129 depletion impaired *Klebsiella* engulfment by MH-S. Similar results were obtained when cells were
15
16 130 treated with filipin and nystatin (Fig. 1B). Since the generation of phosphoinositides is linked to
17
18 131 phagosome formation (Vieira *et al.* 2001), we assessed the contribution of the PI3K signalling
19
20 132 pathway on Kp43816R phagocytosis. Pre-treatment of MH-S cells with LY294002, a specific
21
22 133 inhibitor of PI3K activity, resulted in the blockage of Kp43816R phagocytosis (Fig. 1B). Akt is a
23
24 134 downstream effector of PI3K which becomes phosphorylated upon activation of the PI3K signalling
25
26 135 cascade. As expected, western blot analysis revealed that Kp43816R induces the phosphorylation of
27
28 136 Akt in a PI3K-dependent manner since LY294002 inhibited *Klebsiella*-induced phosphorylation of
29
30 137 Akt (Fig. 1C-D). Similar results were obtained when human macrophages (THP-1 monocytes
31
32 138 differentiated to macrophages by phorbol-12-myristate-13-acetate [PMA] treatment; hereafter
33
34 139 mTHP-1) were infected (Fig. S1).

35
36
37
38
39 140 The bacterial intracellular location in MH-S cells was assessed 3 and 6 h post infection by
40
41 141 transmission electron microscopy (TEM). In good agreement with other published *in vivo*
42
43 142 observations (Cortes *et al.* 2002b, Fevre *et al.* 2013, Willingham *et al.* 2009, Greco *et al.* 2012),
44
45 143 bacteria were located in a vacuolar compartment (Fig. 1E). To determine the fate of intracellular
46
47 144 Kp43816R, MH-S cells were infected with GFP-expressing Kp43816R and the number of
48
49 145 intracellular bacteria was assessed microscopically using differential (inside/outside) staining and
50
51 146 by plating after different incubation times. Bacteria could be clearly observed through the entire
52
53 147 course of infection. To elucidate whether those intracellular bacteria were indeed viable, fluorescent
54
55 148 *in situ* hybridisation (FISH) was carried out by using the oligonucleotide probes EUB338 and
56
57
58
59
60

1
2 149 GAM42a (see Experimental procedures). The detection of bacteria by these oligonucleotide probes
3
4 150 is dependent on the presence of sufficient ribosomes per cell, hence providing qualitative
5
6 151 information on the physiological state of the bacteria on the basis of the number of ribosomes per
7
8 152 cell (Christensen *et al.* 1999, Morey *et al.* 2011). Microscopy analysis revealed that the number of
9
10 153 bacteria metabolically active (FISH positive) *versus* the total number of intracellular bacteria (GFP
11
12 154 positive) was maintained through the infection (Fig. 1F-G). We did not observe any change of host
13
14 155 cell morphology (data not shown). Time course experiments showed that the number of intracellular
15
16 156 bacteria in MH-S cells decreased during the first 2.5 h of infection but then it remained constant
17
18 157 until 8 h post infection (Fig 2A). Immunofluorescence analysis revealed that the phagocytic index
19
20 158 (number of phagocytosed bacteria per 100 macrophages) decreased during the first 2 h and then it
21
22 159 did not change until the end of the experiment (Fig 2B). Similar results were obtained when mTHP-
23
24 160 1 cells were infected (Fig 2C-D).

25
26
27
28 161 Collectively, these results showed that Kp43816R phagocytosis by macrophages is an event
29
30 162 dependent on host cytoskeleton and cell plasma membrane lipid rafts. Moreover, the PI3K/Akt host
31
32 163 signalling pathway is activated by Kp43816R infection and it is required for bacterial phagocytosis.
33
34 164 Our data demonstrate that Kp43816R survives within macrophages through the course of infection
35
36 165 and the TEM experiments suggest that Kp43816R may reside in a specific compartment that we
37
38 166 named the *Klebsiella* containing vacuole (KCV).

39
40
41 167

42 168 ***K. pneumoniae* elicits a cytotoxic effect on macrophages.**

43
44
45
46 169 Examination of the infected monolayers by immunofluorescence at different time points
47
48 170 revealed a decreased in the overall monolayer density at 10 h post infection which was more evident
49
50 171 20 h post infection (Fig S2A). This observation prompted us to study whether Kp43816R exerts a
51
52 172 cytotoxic effect on macrophages. We assessed the viability of infected MH-S cells by measuring the
53
54 173 levels of LDH release. Kp43816R infection was associated with a 35% decrease in cell viability

1 174 after 20 h of infection. Kp43816R-triggered cytotoxic effect on macrophages was also evident when
2
3
4 175 cell viability was estimated by the neutral red uptake assay (Fig S2B).

5
6 176 The induction of host cell apoptosis is one mechanism used by some pathogens to augment
7
8 177 infection (Navarre and Zychlinsky. 2000). To test whether Kp43816R causes apoptosis of MH-S
9
10 178 cells, apoptosis was measured with annexin V, to analyze phosphatidylserine translocation to the
11
12 179 outer leaflet of the plasma membrane, and 7-actinomycin D (AAD) to evaluate plasma membrane
13
14 180 integrity. Flow cytometry analysis of infected cells showed a significant increased in annexin
15
16 181 V⁺AAD⁻ cells over time (Fig. 3). The amount of double-positive annexinV⁺AAD⁺ cells, which
17
18 182 corresponds to a necrotic-like phenotype, was markedly lower at all times analyzed. These results
19
20 183 indicate phosphatidylserine translocation and intact membrane integrity, a classical apoptotic
21
22 184 phenotype, hence suggesting that Kp43816R triggers apoptosis in macrophages.
23
24
25
26
27

185

28 186 ***K. pneumoniae* prevents phagosome fusion with lysosomes.**

29
30 187 Because Kp43816R is able to survive within macrophages, we hypothesized that *Klebsiella*
31
32 188 must either divert the normal process of phagosome maturation or withstand the hostile
33
34 189 environment of the mature phagolysosome. Therefore, we analyzed the maturation of the KCV
35
36 190 during the course of an infection. We analysed the association of the KCV with compartments of
37
38 191 the exocytic pathway. Bacteria did not colocalize with either markers of the endoplasmic reticulum
39
40 192 (calnexin) or markers of the Golgi network (GM 130) at any time analyzed (Fig S3). Next, we
41
42 193 examined the presence on the KCV of markers specific of the successive stations of the endocytic
43
44 194 pathway. EEA1 is an early endosome-specific peripheral membrane protein which colocalizes with
45
46 195 the small GTP binding protein Rab5 (Vieira *et al.* 2002, Flannagan *et al.* 2012). As shown in Figure
47
48 196 4, by 15 min post infection we could detect the presence of EEA1 on 22 ± 4% of KCVs. EEA1 was
49
50 197 lost from KCVs as the percentage of vacuoles positive for this marker dropped to 15% ± 9% and
51
52 198 5% ± 1% at 60 and 90 min post infection, respectively (Fig 4). We next sought to determine
53
54 199 whether the KCV acquires the late endosomal markers Lamp1 and Rab7 (Vieira *et al.*
55
56
57
58
59
60

1
2 200 2002, Flannagan *et al.* 2012). KCVs were positive for Lamp1 already at 30 min post infection and
3
4 201 the percentage of positive KCVs increased over time. KCVs remained positive for Lamp1 until 8 h
5
6 202 post infection. Rab7 is a small G-protein that controls vesicular transport to late endosomes and
7
8 203 lysosomes in the endocytic pathway (Rink *et al.* 2005). To assess the presence of Rab7 on KCVs,
9
10 204 macrophages were transfected with GFP-Rab7 and then infected with Kp43816R. The majority of
11
12 205 the vacuoles containing Kp43816R were positive for Rab7. To determine the activation status of
13
14 206 Rab7 we asked whether RILP, a Rab7 effector protein that exclusively recognizes the active (GTP
15
16 207 bound) conformation of the GTPase (Cantalupo *et al.* 2001, Jordens *et al.* 2001), labels the KCV.
17
18 208 Before infection, cells were transfected with a plasmid containing GFP fused to the C-terminal
19
20 209 Rab7-binding domain of RILP, called “RILP-C33”, which can be used as a reliable index of the
21
22 210 presence and distribution of active Rab7 (Cantalupo *et al.* 2001, Jordens *et al.* 2001). As shown in
23
24 211 Figure 4 RILP-C33-EGFP colocalized with the majority of KCVs.

25
26
27
28 212 Since the interaction of Rab7 with RILP drives fusion with lysosomes (Cantalupo *et al.*
29
30 213 2001, Jordens *et al.* 2001), we sought to determine whether KCV colocalizes with lysosomal
31
32 214 markers. Although there are not markers that unambiguously distinguish late endosomes from
33
34 215 lysosomes, mounting evidence indicates that an acidic luminal pH and the presence of hydrolytic
35
36 216 proteases, such as processed cathepsin D, are characteristics of the phagolysosomal fusion (Vieira *et*
37
38 217 *al.* 2002, Flannagan *et al.* 2012). We used the fixable acidotropic probe LysoTracker to monitor
39
40 218 acidic organelles in infected macrophages. We found a major overlap between the dye and the
41
42 219 KCVs (Fig 5), hence indicating that the KCV is acidic. We next examined the presence in the
43
44 220 vacuole of cathepsin D as a marker for the lysosomal soluble content. However, the majority of the
45
46 221 KCVs did not colocalize with cathepsin D (Fig 5), thereby suggesting that the KCV does not fuse
47
48 222 with lysosomes. To further sustain this notion, we assessed colocalization of the KCV with
49
50 223 tetramethylrhodamine-labelled dextran (TR-dextran). Prior to bacterial infection macrophages were
51
52 224 pulsed with TR-dextran for 2 h followed by a 1 h chase in dye-free medium to ensure that the probe
53
54 225 is delivered from early and recycling endosomes to phagolysosomes (Morey *et al.* 2011, Eissenberg
55
56
57
58
59
60

1
2 226 *et al.* 1988,Hmama *et al.* 2004,Lamothe *et al.* 2007). Confocal immunofluorescence experiments
3
4 227 showed that the majority of the KCVs did not colocalize with TR-dextran (Fig 5B). In contrast,
5
6 228 when macrophages were infected with UV-killed Kp43816R the majority of the KCVs did
7
8 229 colocalize with cathepsin D and TR-dextran (Fig S4). Collectively, these results strongly support
9
10 230 the notion that KCVs containing alive bacteria prevent the fusion of the vacuole with lysosomes.

11
12 231 Similar findings were obtained when mTHP-1 cells were infected. KCV was not associated
13
14 232 with compartments of the exocytic pathway, either Golgi network or endoplasmic reticulum, but
15
16 233 acquired markers of the endocytic pathway, EEA1 and Lamp1 (Fig S5A). The majority of KCVs
17
18 234 colocalized with LysoTracker (Fig S5A) but they were negative for cathepsin D (Fig S5B). In
19
20 235 contrast, nearly 70% of UV-killed Kp43816R colocalized with cathepsin D after 2 h post infection
21
22 236 (Fig S5B). Altogether, these results indicate that only phagosomes containing UV-killed *Klebsiella*
23
24 237 bacteria fuse with lysosomes in human macrophages.

25
26 238 In summary, these findings suggest that *K. pneumoniae* trafficks inside macrophages within
27
28 239 vacuoles associated to the endocytic pathway, and that living *K. pneumoniae* seem to perturb the
29
30 240 fusion of the KCV with the hydrolases-rich lysosomal compartment.

31
32
33
34
35 241

36 37 242 **Inhibition of compartment acidification affects *K. pneumoniae* intracellular survival.**

38
39 243 Phagosome acidification has been shown to be essential for the intracellular survival of
40
41 244 different pathogens (Morey *et al.* 2011,Ghigo *et al.* 2002,Porte *et al.* 1999). Therefore, we
42
43 245 investigated the effect of inhibiting KCV acidification on *K. pneumoniae* survival. Bafilomycin A₁
44
45 246 is a specific inhibitor of the vacuolar type H⁺-ATPase in cells, and inhibits the acidification of
46
47 247 organelles containing this enzyme, such as lysosomes and endosomes. As expected,
48
49 248 phagolysosomal acidification was sensitive to bafilomycin A₁ treatment (Fig 6A), hence confirming
50
51 249 dependence on the vacuolar H⁺-ATPase. Moreover, bafilomycin A₁ treatment also abrogated the
52
53 250 overlap between Kp43816R and the probe LysoTracker (Fig 6A). To assess the effect of vacuolar
54
55 251 acidification on Kp43816R survival, cells were treated with bafilomycin A₁ at the onset of the
56
57
58
59
60

1
2 252 gentamicin treatment and bacteria were enumerated by plating at different time points. Data shown
3
4 253 in Figure 6C revealed that the number of intracellular Kp43816R decreased in bafilomycin A₁
5
6 254 treated cells over time compared to infected untreated cells. Control experiments revealed that
7
8 255 bafilomycin A₁ has no toxic effect on *K. pneumoniae* (our control experiments [data not shown]) or
9
10 256 on other Gram-negative bacteria (Morey *et al.* 2011,Porte *et al.* 1999)). Altogether, these
11
12 257 observations suggest that Kp43816R intracellular survival is dependent on KCV acidification.
13
14
15
16

258

259 **PI3K-AKT and Rab14 aid intracellular survival of *K. pneumoniae*.**

17
18
19 260 *S. enterica* serovar *typhimurium* perturbs the fusion of the phagosomes with lysosomes by
20
21 261 activating the host kinase Akt (Kuijl *et al.* 2007). In turn, inhibition of Akt activation reduces the
22
23 262 intracellular survival of *Salmonella* (Kuijl *et al.* 2007,Chiu *et al.* 2009). Several pathogens also
24
25 263 target the PI3K-Akt axis to manipulate cell biology for their own benefit (Krachler *et al.* 2011).
26
27 264 Since Kp43816R induced the activation of Akt in a PI3K-dependent manner we sought to determine
28
29 265 the contribution of the PI3K-Akt axis to the intracellular survival of *K. pneumoniae*. Treatment of
30
31 266 cells with the PI3K inhibitor LY294002 or the Akt inhibitor AKT X at the onset of the gentamicin
32
33 267 treatment reduced the number of intracellular bacteria in MH-S cells (Fig 7A). Moreover, pulse-
34
35 268 chase experiments revealed that more than 70% bacteria colocalized with TR-dextran in cells
36
37 269 treated with the Akt inhibitor (Fig 7B). Collectively, these results support the notion that Kp43816R
38
39 270 targets the PI3K-Akt axis to survive intracellularly.
40
41
42
43

44 271 At least 18 Rab GTPases are implicated in phagosomal maturation (Smith *et al.* 2007).
45
46 272 Interestingly, *Salmonella* targets Rab14 to prevent phagosomal maturation in an Akt dependent
47
48 273 manner (Kuijl *et al.* 2007). We speculated that Kp43816R may also target Rab14 to control the
49
50 274 maturation of the phagosome. Immunofluorescence experiments revealed that GFP-Rab14
51
52 275 colocalized with the majority of the KCVs (Fig 7C). To determine whether recruitment of Rab14 is
53
54 276 required for intracellular survival cells were transfected with a Rab14 dominant-negative construct
55
56 277 (DN-Rab14) or control vector and then infected with Kp43816R. As shown in figure 7D, we found
57
58
59
60

1
2 278 a 60% decrease in the number of intracellular bacteria in cells transfected with DN-Rab14.
3
4 279 Altogether, these results support the notion that Kp43816R recruits Rab14 to the KCV to control
5
6 280 the maturation of the phagosome.
7

8 281 In summary, our results are consistent with a model where Kp43816R targets the PI3K-Akt-
9
10 282 Rab14 axis to control the phagosome maturation to survive inside macrophages.
11

12 283

13
14
15 284 ***K. pneumoniae* capsule polysaccharide is dispensable for intracellular survival.**
16

17 285 We were keen to identify *K. pneumoniae* factors necessary for intracellular survival. Given
18
19 286 the importance of *K. pneumoniae* CPS on host-pathogen interactions, we explored whether CPS is
20
21 287 also necessary for *K. pneumoniae* intracellular survival. As anticipated, a CPS mutant was engulfed
22
23 288 by MH-S and mTHP1 macrophages in higher numbers than Kp43816R (data not shown). For the
24
25 289 sake of comparison with the wild-type strain in time-course experiments, we adjusted the MOI of
26
27 290 the CPS mutant to get comparable numbers of intracellular bacteria at the beginning of the
28
29 291 infection. Time course experiments showed no differences between the number of intracellular
30
31 292 bacteria of both strains in MH-S and mTHP1 cells (Fig 8A).
32
33

34
35 293 Given the critical role of CPS in preventing complement-mediated opsonophagocytosis
36
37 294 (Alvarez *et al.* 2000, de Astorza *et al.* 2004, Cortes *et al.* 2002a), we evaluated whether the
38
39 295 intracellular fate of the CPS mutant could be modified by bacterial opsonization with human serum.
40
41 296 In agreement with previous reports (de Astorza *et al.* 2004, Cortes *et al.* 2002a), opsonization of the
42
43 297 CPS mutant resulted in an increase in the number of ingested bacteria by mTHP1 cells compared to
44
45 298 nonopsonized bacteria (Fig 8B). For the sake of comparison, the MOI was adjusted to get
46
47 299 comparable numbers of intracellular bacteria at the beginning of the infection. The number of CFU
48
49 300 recovered from cells infected with the opsonized CPS mutant was significantly lower than the
50
51 301 number of CFU recovered from cells infected with non-opsonized bacteria (100 fold lower at 8 h
52
53 302 post infection; Fig 8C). These data indicate that internalization via the C3 receptor results in a
54
55
56
57
58
59
60

1
2 303 significant loss of intracellular viability, presumably because these bacteria are ultimately delivered
3
4 304 to lysosomes.

5
6 305 The lack of contribution of CPS to intracellular survival prompted us to analyze the
7
8 306 expression of *cps* in the KCV. To monitor *cps* expression over time, we constructed a
9
10 307 transcriptional fusion in which the *cps* promoter region was cloned upstream a promoterless *gfp* that
11
12 308 encodes a protein tagged at the C terminus with the (LVA) peptide. The GFP(LVA) protein is
13
14 309 targeted for Tsp protease degradation within the bacteria and has been reported to have 40-min half-
15
16 310 life, while untagged GFP is very stable (estimated *in vivo* half-life, 24 h) (Miller *et al.* 2000).
17
18 311 Kp43816R containing the unstable GFP reporter was used to infect MH-S. Control experiments
19
20 312 showed that there were no differences in the number of intracellular bacteria recovered over time
21
22 313 from cells infected with bacteria containing the reporter plasmid, the empty vector or no plasmid
23
24 314 (data not shown). Cells were lysed, processed as described in Experimental procedures, and
25
26 315 analyzed for fluorescence by FACS at different time points post infection. As shown in Figure 8D,
27
28 316 GFP fluorescence decreased over time reaching the levels of the control strain carrying the empty
29
30 317 vector. To explore whether the acidic pH of the KCV might be responsible for the downregulation
31
32 318 of *cps* expression, bacteria were grown in M9 minimal medium, with different magnesium
33
34 319 concentrations, buffered to different pHs. The expression of the *cps::gfp* fusion was 5-fold lower
35
36 320 when bacteria were grown at pH 5.5 (Fig 8E).
37
38
39
40
41

42 321 Collectively, these findings show that *K. pneumoniae* CPS is dispensable for intracellular
43
44 322 survival. Furthermore, the environment found by *Klebsiella* within the KCV triggers the
45
46 323 downregulation of the expression of *cps*. The fact that opsonization affects the intracellular survival
47
48 324 of the CPS mutant indicates that the mechanism of bacteria entry into macrophages has a major
49
50 325 impact in the ability of *K. pneumoniae* to survive intracellularly.
51

52 326

53 327

54 328

55

56

57

58

59

60

329 **DISCUSSION**

330 In this work, we present compelling evidence demonstrating that *K. pneumoniae* survives
331 killing by macrophages by manipulating phagosome maturation. Our data sustain that *K.*
332 *pneumoniae* traffics within vacuoles associated with the endocytic pathway in mouse and human
333 macrophages. In contrast to UV-killed bacteria, which colocalize with lysosomal markers, alive
334 bacteria modify the vacuole biogenesis preventing the fusion of the KCV with the hydrolases-rich
335 lysosomal compartment. *K. pneumoniae* thus increases the list of pathogens able to alter phagosome
336 maturation.

337 Engulfment of *K. pneumoniae* by mouse and human macrophages was dependent on host
338 cytoskeleton, cell plasma membrane lipid rafts and the activation of PI3K which are all commonly
339 needed to engulf pathogens and inert particles such as latex beads (Vieira *et al.* 2002, Flannagan *et*
340 *al.* 2012). TEM analysis suggested that *K. pneumoniae* resides inside a vacuolar compartment and
341 FISH experiments revealed that intracellular *Klebsiella* were metabolically active for a long period
342 of time. Several lines of evidence indicate that *K. pneumoniae* infections are associated with cell
343 death (Willingham *et al.* 2009, Cano *et al.* 2009, Cai *et al.* 2012). In good agreement, in this study
344 we show that *K. pneumoniae* triggers a programmed cell death in macrophages displaying features
345 of apoptosis. Of note, kinase activity profiling in whole lungs during *K. pneumoniae* infection
346 showed the activation of kinases associated to induction of apoptosis (Hoogendijk *et al.* 2011).
347 However, Willingham and co-workers have reported recently that *K. pneumoniae* activates the
348 NLRP3-dependent cell death programme termed pyronecrosis (Willingham *et al.* 2009). Similar
349 contradictory findings have been reported for *Shigella flexneri* infections. *Shigella* triggers
350 apoptotic and pyroptotic cell death in macrophages depending on the bacterial dosage and time of
351 infection (Willingham *et al.* 2007, Hilbi *et al.* 1998). In the case of *Shigella*, shorter time of contact
352 and low MOI are associated to induction of apoptosis (Willingham *et al.* 2007, Hilbi *et al.* 1998).
353 Notably, the infection conditions in our study are different to those used by Willingham and co-

1
2 354 workers who used a MOI four times higher than ours (Willingham *et al.* 2009). Future studies are
3
4 355 warranted to carefully assess the influence of infection conditions on *Klebsiella*-induced cell death.
5

6 356 The vacuole of *K. pneumoniae* and its biogenesis was studied by immunofluorescence. The
7
8 357 presence of EEA1 on the KCV indicates that internalized bacteria are initially present in a vacuole
9
10 358 related to the endocytic pathway. However, *K. pneumoniae* does not remain in early endosomes as
11
12 359 demonstrated by the acquisition of Lamp1 and Rab7. A hallmark of the maturation is the exclusion
13
14 360 of lysosomal hydrolases in the majority of KCVs containing live bacteria. In contrast, more than
15
16 361 50% of the KCVs containing UV-killed bacteria were positive for lysosomal markers already 90
17
18 362 min post infection. The KCV is acidic most likely due to the activity of vacuolar proton-ATPases.
19
20 363 Notably, inhibition of these pumps by bafilomycin A₁ resulted in a decrease in intracellular
21
22 364 bacterial numbers. Similar findings have been reported for non typable *H. influenzae*, *Tropheryma*
23
24 365 *whipplei*, and *Brucella suis* (Morey *et al.* 2011, Ghigo *et al.* 2002, Porte *et al.* 1999). The reduction
25
26 366 of intracellular viability may have several explanations. Bafilomycin A₁ might affect other cellular
27
28 367 functions necessary for *K. pneumoniae* survival. An alternative hypothesis, and more appealing to
29
30 368 us, is that *K. pneumoniae* requires a low pH environment for survival within the KCV. For example,
31
32 369 the acidic environment may facilitate the uptake of nutrients by *Klebsiella*. Acidic pH is required
33
34 370 for the transport of glucose in *Coxiella burnetii* (Howe and Mallavia. 2000) and localization in an
35
36 371 acidic environment facilitates the availability of iron for the growth of *Francisella tularensis*
37
38 372 (Fortier *et al.* 1995). In addition, low pH may regulate the expression of factors essential for
39
40 373 intracellular survival. This has been shown to be true for virulence gene transcription in *S.*
41
42 374 *typhimurium* (Yu *et al.* 2010). In this context, our data have revealed that *Klebsiella* downregulates
43
44 375 the expression of *cps* when residing within the KCV. Interestingly, when *Klebsiella* was cultured in
45
46 376 low magnesium and acidic pH we also found a downregulation of *cps* expression. It is tempting to
47
48 377 speculate that these signals could trigger *cps* downregulation within the KCV. In fact, in this work
49
50 378 we have shown that the KCV is acidic and there are reports suggesting that the magnesium
51
52 379 concentration in pathogen-containing vacuoles is in the micromolar range (Garcia-del Portillo *et al.*
53
54
55
56
57
58
59
60

1 380 1992). Future efforts will be devoted to characterize the chemical composition of the KCV as well
2
3
4 381 as the transcriptional landscape of intracellular *K. pneumoniae*.

5
6 382 It was interesting to consider the mechanism(s) whereby *K. pneumoniae* prevents the fusion
7
8
9 383 of the lysosomes to the KCV. The overall resemblance between the KCV and the *Salmonella*
10
11 384 containing vacuole (acidic Lamp-1-positive cathepsin-negative vacuole) prompted us to explore
12
13 385 whether *K. pneumoniae* employs similar strategies as *Salmonella* to subvert phagosome maturation.
14
15 386 Kuijl and coworkers (Kuijl *et al.* 2007) demonstrated that *S. typhimurium* activates Akt to prevent
16
17 387 phagosome-lysosome fusion. Since *K. pneumoniae* activates Akt *in vitro* (this work and (Frank *et*
18
19 388 *al.* 2013)) and *in vivo* (Hoogendijk *et al.* 2011) we speculated that activated Akt may also promote
20
21 389 *Klebsiella* intracellular survival. Indeed this was the case. Akt inhibition resulted in a significant
22
23 390 decrease in bacterial intracellular survival associated with an increased colocalization of the KCV
24
25 391 with lysosomal markers. The fact that Akt is implicated in the intracellular survival of other
26
27 392 pathogens, including *M. tuberculosis* (Kuijl *et al.* 2007), strongly suggests that this kinase is a
28
29 393 central host node targeted by pathogens to take control over cellular functions.

30
31
32
33 394 PI3K/Akt governs phagosome maturation by controlling, at least, the activation of Rab
34
35 395 GTPases (Thi and Reiner. 2012), although Rab14 is emerging as a central Rab in this process.
36
37 396 Recent data indicate that pathogens hijack Rab14 to manipulate phagosome maturation. The *M.*
38
39 397 *tuberculosis* vacuole recruits and retains Rab14 to maintain early endosomal characteristics (Kyei *et*
40
41 398 *al.* 2006) whereas *S. typhimurium* containing vacuole retains Rab14 in an Akt-dependent manner to
42
43 399 arrest phagosome maturation (Kuijl *et al.* 2007). Immunofluorescence experiments confirmed that
44
45 400 the KCV is positive for Rab14 whereas transient transfection of the dominant-negative Rab14
46
47 401 resulted in a decrease in bacteria intracellular survival. In aggregate, this evidence supports a
48
49 402 scenario in which *K. pneumoniae* manipulates phagosome maturation by targeting a PI3K-Akt-
50
51 403 Rab14 pathway. Nevertheless, we do not rule out that there are additional pathways necessary for
52
53 404 *Klebsiella* intracellular survival.
54
55
56
57
58
59
60

1
2 405 We were keen to identify the bacterial factors interfering with the phagosomal maturation
3
4 406 pathway. Given the critical role of *K. pneumoniae* CPS in preventing host defense responses (March
5
6 407 *et al.* 2013, Regueiro *et al.* 2006, Lawlor *et al.* 2005, Frank *et al.* 2013, Moranta *et al.* 2010, Campos *et*
7
8 408 *al.* 2004, Lawlor *et al.* 2006), we hypothesized that CPS is necessary for intracellular survival. To
9
10 409 our initial surprise, CPS does not play a large role, if any, in intracellular survival of *Klebsiella*
11
12 410 since a *cps* mutant did not display any loss of viability upon phagocytosis. Furthermore, the *cps*
13
14 411 mutant also triggered a programmed cell death in macrophages (data not shown). Altogether, these
15
16 412 findings may seem contradictory with the well establish role of CPS in *K. pneumoniae* virulence.
17
18 413 However, considering the presence of complement in the bronchoalveolar fluid (Wu *et al.* 2005),
19
20 414 the fact that opsonization results in more efficient internalization of pathogens and maturation of
21
22 415 phagosomes (Aderem and Underhill. 1999), and the well-known role of CPS in preventing
23
24 416 complement opsonization (de Astorza *et al.* 2004, Cortes *et al.* 2002a), we hypothesized that
25
26 417 opsonization of the mutant is deleterious to its intracellular fate. Indeed, this was the case hence
27
28 418 revealing the critical role of CPS on *Klebsiella*-macrophage interplay. These results also illustrate
29
30 419 how the mode of entry of a pathogen influences its intracellular outcome. Similar findings have
31
32 420 been reported for other pathogens (Geier and Celli. 2011, Gordon *et al.* 2000, Drevets *et al.* 1993) but
33
34 421 it cannot be considered a general feature since complement opsonization does not affect the
35
36 422 intracellular fate of *Salmonella* and *M. tuberculosis* (Drecktrah *et al.* 2006, Zimmerli *et al.* 1996).

37
38 423 Finally, it is worthwhile commenting on the clinical implications of this study. The
39
40 424 antibiotics commonly used to treat *Klebsiella* infections are not very efficient against intracellular
41
42 425 bacteria. In turn, our findings provide rationale for the use of inhibitors targeting the PI3K-Akt
43
44 426 signaling cascade to eliminate intracellular *K. pneumoniae*. The concept of eradicating pathogens
45
46 427 through targeting host factors modulated by pathogens has received wide attention in the infectious
47
48 428 disease arena. Several promising drugs have been developed or are being developed to antagonize
49
50 429 PI3K/Akt due to its relevance for many human cancers. Of note, there are *in vitro* and *in vivo*
51
52 430 studies supporting the use of Akt inhibitors to eliminate intracellular *Salmonella* and *M.*

1 431 *tuberculosis* (Kuijl *et al.* 2007, Chiu *et al.* 2009). Therefore, we propose that agents targeting
2
3 432 PI3K/Akt might provide selective alternatives to manage *K. pneumoniae* pneumonias. Careful
4
5
6 433 designed preclinical trials using the well establish mouse pneumonia model are warranted to test
7
8 434 this hypothesis.
9

10 435

11 436 **EXPERIMENTAL PROCEDURES**

12 437 **Bacterial strains and growth conditions.**

13
14
15
16
17 438 Kp43816R is a rifampicin-resistant derivative of *K. pneumoniae* pneumonia clinical isolate
18
19 439 expressing a type 1 O-polysaccharide and a type 2 capsule (ATCC 43816). Bacteria were grown in
20
21 440 lysogeny broth (LB) at 37°C on an orbital shaker (180 rpm). To UV kill bacteria, samples were UV
22
23 441 irradiated (1 joule for 15 min) in a BIO-LINK BLX crosslinker (Vilber Lourmat). When
24
25 442 appropriate, antibiotics were added to the growth medium at the following concentrations:
26
27 443 rifampicin (Rif) 50 µg/ml, ampicillin (Amp), 100 µg/ml for *K. pneumoniae* and 50 µg/ml for *E.*
28
29 444 *coli*; kanamycin (Km) 100 µg/ml; chloramphenicol (Cm) 12.5 µg/ml.
30
31

32 445 **Construction of a *K. pneumoniae cps* mutant.**

33
34
35 446 Primers for *manC* mutant construction were designed from the known *K. pneumoniae* K2
36
37 447 gene cluster sequence (Arakawa *et al.* 1995). Primer pairs ManCUPF (5'-
38
39 448 CGCTTAAAGACCAGCGTGTCG -3'), ManCUPR (5'-
40
41 449 CGGATCCGATCAGCGGGTCGTCGCCGTG____-3'), and ManCDOWNF (5'-
42
43 450 CGGATCCGCAGCGACGAGAAGCTGGTGG-3' *Bam*HI site underlined), ManCDOWNR (5'-
44
45 451 GGATATCCCGCAGGCCGGTG -3') were used in two sets of asymmetric PCRs to obtain DNA
46
47 452 fragments ManCUP and ManCDown, respectively. DNA fragments ManCUP and ManCDOWN
48
49 453 were annealed at their overlapping region and amplified by PCR as a single fragment using primers
50
51 454 ManCUPF and ManCDOWNR. This PCR fragment was cloned into pGEM-T Easy to obtain
52
53 455 pGEMTΔ*manC*. A kanamycin cassette, obtained as a 1.5 kb PCR fragment from pKD4 (Datsenko
54
55 456 and Wanner. 2000) using primers cassette-F1 (5'-
56
57
58
59
60

1
2 457 CGCGGATCCGTGTAGGCTGGAGCTGCTTCG-3' *Bam*HI site underlined) and cassette-R1 (5'-
3
4 458 CGCGGATCCCATGGGAATTAGCCATGGTCC -3' *Bam*HI site underlined), was BamHI-
5
6 459 digested and cloned into BamHI-digested pGEMT Δ *manC* to obtain pGEMT Δ *manCKm*. Primers
7
8 460 ManCUPF and ManCDOWNR were used to amplify a 3.5 kb fragment which was electroprated
9
10 461 into Kp43816R containing pKOBEG-*sacB* plasmid (Derbise *et al.* 2003). The vector pKOBEG-
11
12 462 *sacB* contains the Red operon expressed under the control of the arabinose inducible pBAD
13
14 463 promoter and the *sacB* gene that is necessary to cure the plasmid. A recombinant in which the wild-
15
16 464 type allele was replaced by Δ *man::Km* was verified by PCR and named 43 Δ *manCKm*. The mutant
17
18 465 was resistant to the CPS-specific phage ϕ 2.
19

20 466 **Eukaryotic cells culture.**

21
22
23
24 467 Murine alveolar macrophages MH-S (ATCC, CRL-2019) and human monocytes THP-1
25
26 468 (ATCC, TIB-202) were grown in RPMI 1640 tissue culture medium supplemented with 10% heat-
27
28 469 inactivated fetal calf serum (FCS) and 10 mM Hepes at 37°C in an humidified 5% CO₂ atmosphere.
29
30 470 THP-1 cells were differentiated to macrophages by PMA-treatment (10 ng/ml for 12 h).
31
32

33 471 **Infection of macrophages.**

34
35 472 Macrophages were seeded in 24-well tissue culture plates at a density of 7×10^5 cells per
36
37 473 well 15 h before the experiment. Bacteria were grown in 5-ml LB, harvested in the exponential
38
39 474 phase (2500 x g, 20 min, 24°C), washed once with PBS and a suspension containing approximately
40
41 475 1×10^9 cfu/ml was prepared in 10 mM PBS (pH 6.5). Cells were infected with 35 μ l of this
42
43 476 suspension to get a multiplicity of infection of 50:1 in a final volume of 500 μ l RPMI 1640 tissue
44
45 477 culture medium supplemented with 10% heat-inactivated FCS and 10 mM Hepes. To synchronize
46
47 478 infection, plates were centrifuged at 200 x g during 5 min. Plates were incubated at 37°C in a
48
49 479 humidified 5% CO₂ atmosphere. After 30 min of contact, cells were washed twice with PBS and
50
51 480 incubated for additional 90 min with 500 μ l RPMI 1640 containing 10% FCS, 10 mM Hepes,
52
53 481 gentamicin (300 μ g/ml) and polymyxin B (15 μ g/ml) to eliminate extracellular bacteria. This
54
55 482 treatment did not induce any cytotoxic effect which was verified measuring the release of lactate
56
57
58
59
60

1
2 483 dehydrogenase (LDH) and by immunofluorescence microscopy (data not shown). For time course
3
4 484 experiments, after the 90 min treatment period, cells were washed three times with PBS and
5
6 485 incubated with 500 μ l RPMI 1640 containing 10% FCS, 10 mM Hepes, gentamicin (100 μ g/ml).
7

8
9 486 To determine intracellular bacterial load, cells were washed three times with PBS and lysed
10
11 487 with 300 μ l of 0.5% saponin in PBS for 10 min at room temperature. Serial dilutions were plated on
12
13 488 LB to quantify the number of intracellular bacteria. Intracellular bacterial load is represented as cfu
14
15 489 per well. All experiments were done with triplicate samples on at least three independent occasions.
16

17
18 490 When indicated, cells were pre-incubated for 1 h with nocodazole (50 μ g/ml), filipin (5
19
20 491 μ g/ml), nystatin (25 μ g/ml), LY294002 hydrochloride (75 μ M), or for 30 min with cytochalasin D
21
22 492 (5 μ g/ml) before carrying out infections as described above. Cells were also pre-incubated for 1 h
23
24 493 with 1 mM methyl- β -cyclodextrin (M β CD), washed twice with PBS to remove cholesterol and
25
26 494 infected. In other experiments, LY294002 hydrochloride (75 μ M), AKT X (10 μ M), or 100 nM
27
28 495 bafilomycin A₁ were added to the cells during the gentamicin treatment and kept until the end of
29
30 496 experiment. All drugs were purchased from Sigma.
31
32

33 497 **Immunofluorescence and transmission electron microscopy.**

34
35 498 Cells were seeded on 12 mm circular coverslips in 24-well tissue culture plates. Infections
36
37 499 were carried out as described before with *K. pneumoniae* strains harbouring pFPV25.1Cm (March
38
39 500 *et al.* 2013). Control experiments showed that there were no differences in the number of
40
41 501 intracellular bacteria recovered over time from cells infected with bacteria containing pFPV25.1Cm
42
43 502 or no plasmid (data not shown). When indicated, cells were washed three times with PBS and fixed
44
45 503 with 3% paraformaldehyde (PFA) in PBS pH 7.4 for 15 min at room temperature. For EEA1
46
47 504 staining, cells were fixed with 2.5% PFA for 10 min at room temperature followed by 5% PFA +
48
49 505 methanol (1:4 v/v) at -20°C for 5 min. Methanol fixation (3% PFA for 20 min at room temperature
50
51 506 followed by 1 min cold methanol) was used for cathepsin D whereas periodate-lysine-
52
53 507 paraformaldehyde fixation (0.01 M NaIO₄, 0.075 M L-lysine, 0.0375 M NaPO₄ buffer pH 7.4, 2%
54
55 508 paraformaldehyde: 20 min room temperature) was used for calnexin. The actin cytoskeleton was
56
57
58
59
60

1
2 509 stained with Rhodamine-Phalloidin (Invitrogen) diluted 1:100, DNA was stained with Hoechst
3
4 510 33342 (Invitrogen) diluted 1:2500. *Klebsiella* was stained with rabbit anti-*Klebsiella* serum diluted
5
6 511 1:5000. Early endosomes were stained with goat anti-EEA1 (N-19) antibody (Santa Cruz
7
8 512 Biotechnology) diluted 1:50. Late endosomes were stained with rat anti-Lamp-1 (1D4B) antibody
9
10 513 (Developmental Studies Hybridoma Bank). Lysosomes were labelled with goat anti-human
11
12 514 cathepsin D (G19) or rabbit anti-human cathepsin D (H-75) antibodies (Santa Cruz Biotechnology)
13
14 515 diluted 1:100. Golgi network was stained with mouse anti-GM130 (BD Laboratories) diluted 1:400.
15
16 516 Endoplasmic reticulum was stained with rabbit anti-calnexin (SPA-860; Enzo Life Sciences) diluted
17
18 517 1:400. Donkey anti-rabbit, donkey anti-mouse, donkey anti-rat and donkey anti-goat conjugated to
19
20 518 Rhodamine, Cy5 or Cy2 secondary antibodies were purchased from Jackson Immunological and
21
22 519 diluted 1:200.
23
24
25

26
27 520 Fixable dextran 70,000 (molecular weight) labelled with Texas red (TR-dextran) (Molecular
28
29 521 Probes) was used to label lysosomes in a pulse-chase assay. Briefly, macrophages seeded on glass
30
31 522 coverslips were labelled by pulsing with 250 $\mu\text{g}/\text{ml}$ of TR-dextran for 2 h at 37°C in 5% CO₂ in
32
33 523 RPMI 1640 medium. To allow TR-dextran to accumulate in lysosomes, medium was removed; cells
34
35 524 were washed three times with PBS, and incubated for 1 h in dye-free medium (chase). After the
36
37 525 chase period, cells were infected. Acidic compartments were loaded with 0.5 μM LysoTracker
38
39 526 RedDN99 (Invitrogen), 45 min before fixation. At the end of the infection period, the residual fluid
40
41 527 marker was removed by washing the cells three times with PBS, followed by fixation.
42
43
44

45 528 Staining was carried out in 10% horse serum, 0.1% saponin in PBS. Coverslips were washed
46
47 529 twice in PBS containing 0.1% saponin, once in PBS, and incubated for 30 minutes with primary
48
49 530 antibodies. Coverslips were then washed twice in 0.1% saponin in PBS and once in PBS and
50
51 531 incubated for 30 minutes with secondary antibodies. Finally, coverslips were washed twice in 0.1%
52
53 532 saponin in PBS, once in PBS and once in H₂O, mounted on Aqua Poly/Mount (Polysciences) and
54
55 533 analysed with a Leica TCS SP5 confocal microscope. Depending of the marker, a KCV was
56
57 534 considered positive when it fulfilled these criteria: (i) the marker was detected throughout the area
58
59
60

1
2 535 occupied by the bacterium; (ii) the marker was detected around/enclosing the bacterium, (iii) the
3
4 536 marker was concentrated in this area, compared to the immediate surroundings. To determine the
5
6 537 percentage of bacteria that colocalized with each marker, all bacteria located inside a minimum of
7
8 538 100 infected cells were analysed in each experiment. Experiments were carried out by triplicate in
9
10 539 three independent occasions.

11
12 540 For extra-/intracellular bacteria differential staining, PFA fixed cells were incubated with
13
14 541 PBS containing 10% horse serum, Hoechst 33342 and rabbit anti-*Klebsiella* for 20 min. Coverslips
15
16 542 were washed three times with PBS and stained as described above with donkey anti-rabbit
17
18 543 conjugated to Rhodamine secondary antibody. Coverslips were washed three times in PBS and once
19
20 544 in distilled water before mounting onto glass slides using Prolong Gold antifade mounting gel
21
22 545 (Invitrogen).

23
24 546 Immunofluorescence was analysed with a Leica CTR6000 fluorescence microscope. Images
25
26 547 were taken with a Leica DFC350FX monochrome camera. Confocal microscopy was carried out
27
28 548 with a Leica TCS SP5 confocal microscope.

29
30 549 For transmission electron microscopy (TEM), cells were seeded in 24-well tissue culture
31
32 550 plates. Infections were carried out as described before, fixed with glutaraldehyde and processed for
33
34 551 TEM as described previously (Kruskal *et al.* 1992).

35 552 **Fluorescent *in situ* hybridisation**

36
37 553 We carried out hybridization of PFA fixed infected cells with fluorescently labelled
38
39 554 oligonucleotides as described before (Morey *et al.* 2011). Alexa488 conjugated DNA probes
40
41 555 EUB338 (5'-GCTGCCTCCCGTAGGAGT-3') and GAM42a (5'-GCCTTCCCACATCGTTT-3')
42
43 556 were designed for specific labelling of rRNA of eubacteria and gamma subclass of Proteobacteria,
44
45 557 respectively (Manz *et al.* 1993). A DNA probe non-EUB338, complementary to EUB338 was used
46
47 558 as a negative control. The detectability of bacteria by such oligonucleotide probes is dependent on
48
49 559 the presence of sufficient ribosomes per cell, hence providing qualitative information on the
50
51 560 physiological state of the bacteria on the basis of the number of ribosomes per cell. These probes
52
53
54
55
56
57
58
59
60

1
2 561 were used together to obtain a stronger signal, added to a final concentration of 5 nM each in the
3
4 562 hybridization buffer. The hybridization buffer contained 0.9M NaCl, 20mM Tris-HCl (pH 7.4),
5
6 563 0.01% sodium dodecyl sulfate (SDS) and 35% formamide. Coverslips were first washed with
7
8 564 deionized water. Hybridization was carried out for 1.5 h at 46°C in a humid chamber; followed by a
9
10 565 30 min wash at 48°C. Washing buffer contained 80 mM NaCl, 20 mM Tris-HCl (pH 7.4), 0.01%
11
12 566 sodium dodecyl sulfate (SDS) and 5 mM EDTA (pH 8). After washing, DNA staining for total
13
14 567 bacteria was carried out by incubating the coverslips in PBS containing Hoechst 33342 for 20 min.
15
16 568 Coverslips were then washed three times in PBS and once in distilled water before mounting onto
17
18 569 glass slides using Prolong Gold antifade mounting gel.

21 570 **Isolation of *in vivo* infected macrophages**

22
23
24 571 Mice were treated in accordance with the Directive of the European Parliament and of the
25
26 572 Council on the protection of animals used for scientific purposes (Directive 2010/63/EU) and in
27
28 573 agreement with the Bioethical Committee of the University of the Balearic Islands. This study was
29
30 574 approved by the Bioethical Committee of the University of the Balearic Islands with the
31
32 575 authorisation number 1748.

33
34
35 576 Infections were performed as previously described (Insua *et al.* 2013). Briefly, five- to
36
37 577 seven-week-old male CD-1 mice (Harlan) were anesthetized by intraperitoneal injection with a
38
39 578 mixture containing ketamine (50 mg/kg) and xylazine (5 mg/kg). Overnight bacterial cultures were
40
41 579 centrifuged (2500 x g, 20 min, 22°C), resuspended in PBS and adjusted to 5×10^4 CFU/ml for
42
43 580 determination of bacterial loads. 20 μ l of the bacterial suspension were inoculated intranasally in
44
45 581 four 5 μ l aliquots. To facilitate consistent inoculations, mice were held vertically during inoculation
46
47 582 and placed on a 45° incline while recovering from anaesthesia. 24 h post infection, mice were
48
49 583 euthanized by cervical dislocation and bronchoalveolar lavage was performed as previously
50
51 584 described (Cai *et al.* 2012). The lavage fluid was spun at 300 x g for 10 min to pellet alveolar
52
53 585 macrophages. Cells were cultured on 12 mm circular coverslips in 24-well tissue culture plates at a
54
55 586 concentration of 0.5×10^6 cells/well in 1 ml RPMI 1640 tissue culture medium supplemented with
56
57
58
59
60

1
2 587 10% heat-inactivated FCS and 10 mM Hepes and gentamicin (100 µg/ml). After 2 h of incubation,
3
4 588 nonadherent cells were washed off with PBS, and cells were fixed. *Klebsiella* and cathepsin D
5
6 589 staining was performed as previously described. Immunofluorescence was analysed with a with a
7
8 590 Leica TCS SP5 confocal microscope.

591 **Neutral red uptake assay for the estimation of cell viability.**

592 Cell viability was determined by assessing the ability of viable cells to incorporate and bind
593 the supravital dye neutral red in the lysosomes. The protocol described by Repetto and coworkers
594 (Repetto *et al.* 2008) was followed with minor modifications. Macrophages were seeded on 96-well
595 tissue culture plates at 5×10^5 cells/well 18 h before the experiment. Cells were infected to get a
596 multiplicity of infection of 50:1 in a final volume of 200 µl RPMI 1640 tissue culture medium
597 supplemented with 10% heat-inactivated FCS and 10 mM Hepes. To synchronize infection, plates
598 were centrifuged at 200 x g during 5 min. Plates were incubated at 37°C in a humidified 5% CO₂
599 atmosphere. After 90 min of contact, cells were washed twice with PBS and incubated overnight
600 with 200 µl RPMI 1640 containing 10% FCS, 10 mM Hepes, gentamicin (100 µg/ml). Cells were
601 washed twice with PBS and incubated with 100 µl of freshly prepared neutral red medium (final
602 concentration 40 µg/ml neutral red [Sigma] in tissue culture medium) for 2 h. Wells were washed
603 once with PBS and the remaining biomass-adsorbed neutral red was solubilized with 150 µl neutral
604 red destaining solution (50% ethanol 96%; 49% deionised water, 1% glacial acetic acid). Staining
605 was then quantified by determining the OD₅₄₀ in a 96-well microplate reader, and used to compare
606 relative neutral red staining of uninfected cells and cells that were lysed completely with 1% Triton
607 X-100. Experiments were carried out by triplicate in six independent occasions.

608 **Detection of Akt phosphorylation by Western blotting**

609 Macrophages were seeded on 6-well tissue culture plates at 10^6 cells/well. Cells were
610 infected with Kp43816R, washed 3 times with cold PBS, scraped and lysed with 100 µl lysis buffer
611 (1x SDS Sample Buffer, 62.5 mM Tris-HCl pH 6.8, 2% w/v SDS, 10% glycerol, 50 mM DTT,
612 0.01% w/v bromophenol blue) on ice. Samples were sonicated, boiled at 100°C for 10 min and

1
2 613 cooled on ice before polyacrylamide gel electrophoresis and Western Blotting. Akt phosphorylation
3
4 614 was detected with primary rabbit anti-phospho Ser473 Akt (Cell Signaling Technology) antibody
5
6 615 diluted 1:1,000 and secondary goat anti-rabbit antibody conjugated to horseradish peroxidase
7
8 616 (Thermo Scientific) diluted 1:10,000. Tubulin was detected with primary mouse anti-tubulin
9
10 617 antibody (Sigma) diluted 1:3,000 and secondary goat anti-mouse antibody (Pierce) conjugated to
11
12 618 horseradish peroxidase diluted 1:1,000. When necessary, the membrane was washed twice for 15
13
14 619 min with PBS-0.5% Tween-20, incubated for 30 min in RestoreTM Western Blot Stripping Buffer
15
16 620 (Thermo Scientific) at 37°C, and washed twice for 15 min with PBS-0.5% Tween-20. Images were
17
18 621 recorded with a GeneGnome HR imaging system (Syngene).

22 **Apoptosis analysis *in vitro*.**

23
24 623 Apoptosis of macrophages was analysed as previously described (Aguilo *et al.* 2013).
25
26 624 Briefly, phosphatidylserine exposure and membrane integrity were analyzed by using Annexin-V
27
28 625 and 7-AAD (BD Biosciences) and FACS according to manufacturer instructions. Cells were
29
30 626 washed with PBS and incubated with APC-conjugated Annexin-V and 7-AAD in Annexin-binding
31
32 627 buffer for 15 min. After that, cells were washed twice with PBS, fixed with 4% PFA during 30 min
33
34 628 and washed again with PBS. Both PBS and PFA contained 2.5 mM CaCl₂.

37 **Bacterial opsonisation.**

38
39 630 Normal human serum (NHS), kindly donated by the Balearics Blood Centre, was obtained
40
41 631 from five different donors (blood type O negative) and kept frozen at -80°C. 35 µl from a
42
43 632 suspension containing approximately 1x10⁹ cfu/ml in 10 mM PBS (pH 6.5) were added to 500 µl
44
45 633 RPMI 1640 tissue culture medium supplemented with 10 mM HEPES and 1% NHS. The suspension
46
47 634 was incubated at 37°C shaking (180 rpm) for 45 min. The suspension was used to infect mTHP1
48
49 635 cells as previously described.

53 **Plasmids and transient transfections**

54
55 637 For transient transfections with GFP-Rab7 (Cantalupo *et al.* 2001), GFP-Rab14 (Kuijl *et al.*
56
57 638 2007), and RILP-C33-EGFP (Cantalupo *et al.* 2001), macrophages were seeded in 24-well tissue

1
2 639 culture plates at a density of 3×10^5 cells per well 24 h before transfection. Cells were transfected
3
4 640 with 750 ng DNA using FuGENE (Promega) according to manufacturer's instructions
5
6 641 (reagent/DNA ratio 3.5:1). In all cases, samples were fixed, stained and analysed by
7
8 642 immunofluorescence microscopy. pcDNA3 and DN-Rab14 (Seto *et al.* 2011) were transfected
9
10 643 using jetPEI-macrophage (Polyplus) following manufacturer's instructions. After 24 h, cells were
11
12 644 washed twice with PBS, infected, and intracellular bacterial load determined as previously
13
14 645 described.

17 646 **Construction of *cps* reporter strain**

18
19 647 DNA fragment containing the promoter region of the Kp43816R capsule operon was
20
21 648 amplified by PCR using *Vent* polymerase (NewEngland Biolabs) and primers K2ProcpsF (5'-
22
23 649 gaattcTGCTGGGACAAATTGCCACC-3') and K2ProcpsR (5'-
24
25 650 AGATGGATGACCCCGCGATC-3'). To construct a green fluorescent protein (GFP) reporter, the
26
27 651 PCR product was EcoRI-digested and cloned into the EcoRI-SmaI digested low-copy-number
28
29 652 vector pPROBE'-gfp[LVA] (Miller *et al.* 2000) to obtain pPROBE'43Procps. The plasmid was
30
31 653 introduced into Kp43816R by electroporation.
32
33

34 654 **Analysis of *cps* expression**

35
36 655 The reporter strains were grown at 37°C on an orbital incubator shaker (180 r.p.m.) until
37
38 656 OD₅₄₀ 1.2. The cultures were harvested (2500 x g, 20 min, 24°C) and resuspended to an OD₅₄₀ of
39
40 657 0.6 in PBS. 0.8-ml aliquot of this suspension was transferred to 1-cm fluorimetric cuvette and
41
42 658 fluorescence was measured with a spectrofluorophotometer (Perkin Elmer LS55) set as follows:
43
44 659 excitation, 485 nm; emission, 528 nm; slit width 5 nm; integration time 5 seconds. Results were
45
46 660 expressed as relative fluorescence units (RFU). All measurements were carried out in quintuplicate
47
48 661 on at least three separate occasions.
49
50

51
52 662 For analysis of *cps* expression from intracellular bacteria, macrophages were seeded in 6-
53
54 663 well plates and infected with Kp43816R containing pPROBE'43Procps or pPROBE'-gfp[LVA]
55
56 664 control vector at a MOI of 150:1. After 40 min, cells were washed twice with PBS and incubated
57
58
59
60

1
2 665 with 500 μ l RPMI 1640 containing 10% FCS, 10 mM Hepes, gentamicin (300 μ g/ml) and
3
4 666 polymyxin B (15 μ g/ml) to eliminate extracellular bacteria. At the indicated time points, cells were
5
6 667 lysed with 900 μ l 0.5 % saponin in PBS. The samples from two wells were combined and serial
7
8 668 dilutions were plated on LB to quantify the number of intracellular bacteria. Control experiments
9
10 669 showed that there were no differences in the number of intracellular bacteria recovered over time
11
12 670 from cells infected with bacteria containing pPROBE'-gfp[LVA] derivatives or no plasmid (data
13
14 671 not shown). By replica plating on plates containing kanamycin, it was determined that 85-100% of
15
16 672 the bacteria contained the reporter plasmid at any time point analysed. The rest of the lysate was
17
18 673 centrifuged (13 000 rpm, 1 min, room temperature) and resuspended in 1 ml 1 % BSA in PBS for
19
20 674 staining. Bacteria were stained with rabbit anti-*Klebsiella* serum diluted 1:5000 for 20 min, washed
21
22 675 twice with PBS, and incubated for 20 min with a 1:200 dilution of Rhodamine-conjugated donkey
23
24 676 anti-rabbit secondary antibody. Flow cytometry analyses were performed using a Cultek Epics XL
25
26 677 flow cytometer. Samples were gated for bacteria-like particles by using the rhodamine fluorescence
27
28 678 of the anti-*Klebsiella* labelling to identify bacterial cells and to exclude mammalian cell debris and
29
30 679 background noise. Lysed and stained uninfected macrophages were not rhodamine positive,
31
32 680 indicating that there was no cross-reactivity of the primary or secondary antibodies with MH-S
33
34 681 cells. Fluorescence compensation settings were determined in parallel under identical conditions by
35
36 682 using the constitutively GFP-expressing Kp43816R strain or the non-expressing strain, with and
37
38 683 without anti-*Klebsiella* antibody labelling. Approximately 10,000 events identified as *Klebsiella*
39
40 684 cells were collected per sample. A histogram of GFP fluorescence for the negative-control sample
41
42 685 (bacteria containing pPROBE'-gfp[LVA]) was created, and the area of the histogram containing
43
44 686 the bacterial population was considered to be negative for GFP fluorescence. All experiments were
45
46 687 done with triplicate samples on at least three independent occasions.
47
48
49
50
51
52

53 688 **Statistical analysis.**
54
55
56
57
58
59
60

1
2 689 Statistical analyses were performed using the one-tailed *t* test or, when the requirements
3
4 690 were not met, by the Mann-Whitney U test. $P < 0.05$ was considered statistically significant. The
5
6 691 analyses were performed using Prism4 for PC (GraphPad Software).
7

8
9 692

10 693 **ACKNOWLEDGEMENTS**

11
12 694 We are grateful to members of Bengoechea lab for helpful discussions. We are indebted to Sergio
13
14 695 Grinstein, Jacques Neefjes and Yukio Koide for sending us plasmids and helpful discussions.
15
16 696 M.I.M.-L. was financially supported by the Instituto de Salud Carlos III (grant CM09/000123). Part
17
18 697 of this work was supported by grant PS09-00130 from Instituto de Salud Carlos III to J.G., and by a
19
20 698 grant from Biomedicine Program (SAF2009-07885) from Ministerio de Economía y
21
22 699 Competitividad (Spain); Marie Curie Career Integration Grant U-KARE (PCIG13-GA-2013-
23
24 700 618162); and Queen's University Belfast start-up funds to J.A.B. CIBERES is an initiative from
25
26 701 Instituto de Salud Carlos III.
27
28
29

30
31 702

32 703 **REFERENCES**

- 33
34
35 704 Aderem, A., and Underhill, D.M. (1999) Mechanisms of phagocytosis in macrophages. *Annu Rev*
36 705 *Immunol* 17: 593-623.
- 37
38 706 Aguilo, J.I., Alonso, H., Uranga, S., Marinova, D., Arbues, A., de Martino, A., *et al* (2013) ESX-1-
39 707 induced apoptosis is involved in cell-to-cell spread of *Mycobacterium tuberculosis*. *Cell Microbiol*
40 708 15: 1994-2005.
- 41
42 709 Alvarez, D., Merino, S., Tomas, J.M., Benedi, V.J., and Alberti, S. (2000) Capsular polysaccharide
43 710 is a major complement resistance factor in lipopolysaccharide O side chain-deficient *Klebsiella*
44 711 *pneumoniae* clinical isolates. *Infect Immun* 68: 953-955.
- 45
46 712 Arakawa, Y., Wacharotayankun, R., Nagatsuka, T., Ito, H., Kato, N., and Ohta, M. (1995) Genomic
47 713 organization of the *Klebsiella pneumoniae cps* region responsible for serotype K2 capsular
48 714 polysaccharide synthesis in the virulent strain Chedid. *J Bacteriol* 177: 1788-1796.
- 49
50 715 Broug-Holub, E., Toews, G.B., van Iwaarden, J.F., Strieter, R.M., Kunkel, S.L., Paine, R., 3rd, *et al*
51 716 (1997) Alveolar macrophages are required for protective pulmonary defenses in murine *Klebsiella*
52 717 pneumonia: elimination of alveolar macrophages increases neutrophil recruitment but decreases
53 718 bacterial clearance and survival. *Infect Immun* 65: 1139-1146.
- 54
55 719 Cai, S., Batra, S., Wakamatsu, N., Pacher, P., and Jeyaseelan, S. (2012) NLRC4 inflammasome-
56 720 mediated production of IL-1beta modulates mucosal immunity in the lung against gram-negative
57 721 bacterial infection. *J Immunol* 188: 5623-5635.

- 1
2 722 Campos, M.A., Vargas, M.A., Regueiro, V., Llompart, C.M., Alberti, S., and Bengoechea, J.A.
3 723 (2004) Capsule polysaccharide mediates bacterial resistance to antimicrobial peptides. *Infect Immun*
4 724 72: 7107-7114.
- 5
6 725 Camprubi, S., Merino, S., Benedi, V.J., and Tomas, J.M. (1993) The role of the O-antigen
7 726 lipopolysaccharide and capsule on an experimental *Klebsiella pneumoniae* infection of the rat
8 727 urinary tract. *FEMS Microbiol Lett* 111: 9-13.
- 9
10 728 Cano, V., Moranta, D., Llobet-Brossa, E., Bengoechea, J.A., and Garmendia, J. (2009) *Klebsiella*
11 729 *pneumoniae* triggers a cytotoxic effect on airway epithelial cells. *BMC Microbiol* 9: 156-2180-9-
12 730 156.
- 13
14 731 Cantalupo, G., Alifano, P., Roberti, V., Bruni, C.B., and Bucci, C. (2001) Rab-interacting
15 732 lysosomal protein (RILP): the Rab7 effector required for transport to lysosomes. *EMBO J* 20: 683-
16 733 693.
- 17
18 734 Cheung, D.O., Halsey, K., and Speert, D.P. (2000) Role of pulmonary alveolar macrophages in
19 735 defense of the lung against *Pseudomonas aeruginosa*. *Infect Immun* 68: 4585-4592.
- 20
21 736 Chiu, H.C., Soni, S., Kulp, S.K., Curry, H., Wang, D., Gunn, J.S., *et al* (2009) Eradication of
22 737 intracellular *Francisella tularensis* in THP-1 human macrophages with a novel autophagy inducing
23 738 agent. *J Biomed Sci* 16: 110-0127-16-110.
- 24
25 739 Christensen, H., Hansen, M., and Sorensen, J. (1999) Counting and size classification of active soil
26 740 bacteria by fluorescence in situ hybridization with an rRNA oligonucleotide probe. *Appl Environ*
27 741 *Microbiol* 65: 1753-1761.
- 28
29 742 Cortes, G., Alvarez, D., Saus, C., and Alberti, S. (2002a) Role of lung epithelial cells in defense
30 743 against *Klebsiella pneumoniae* pneumonia. *Infect Immun* 70: 1075-1080.
- 31
32 744 Cortes, G., Borrell, N., de Astorza, B., Gomez, C., Sauleda, J., and Alberti, S. (2002b) Molecular
33 745 analysis of the contribution of the capsular polysaccharide and the lipopolysaccharide O side chain
34 746 to the virulence of *Klebsiella pneumoniae* in a murine model of pneumonia. *Infect Immun* 70: 2583-
35 747 2590.
- 36
37 748 Datsenko, K.A., and Wanner, B.L. (2000) One-step inactivation of chromosomal genes in
38 749 *Escherichia coli* K-12 using PCR products. *Proc Natl Acad Sci U S A* 97: 6640-6645.
- 39
40 750 de Astorza, B., Cortes, G., Crespi, C., Saus, C., Rojo, J.M., and Alberti, S. (2004) C3 promotes
41 751 clearance of *Klebsiella pneumoniae* by A549 epithelial cells. *Infect Immun* 72: 1767-1774.
- 42
43 752 Derbise, A., Lesic, B., Dacheux, D., Ghigo, J.M., and Carniel, E. (2003) A rapid and simple method
44 753 for inactivating chromosomal genes in *Yersinia*. *FEMS Immunol Med Microbiol* 38: 113-116.
- 45
46 754 Drecktrah, D., Knodler, L.A., Ireland, R., and Steele-Mortimer, O. (2006) The mechanism of
47 755 *Salmonella* entry determines the vacuolar environment and intracellular gene expression. *Traffic* 7:
48 756 39-51.
- 49
50 757 Drevets, D.A., Leenen, P.J., and Campbell, P.A. (1993) Complement receptor type 3
51 758 (CD11b/CD18) involvement is essential for killing of *Listeria monocytogenes* by mouse
52 759 macrophages. *J Immunol* 151: 5431-5439.
- 53
54 760 Eissenberg, L.G., Schlesinger, P.H., and Goldman, W.E. (1988) Phagosome-lysosome fusion in
55 761 P388D1 macrophages infected with *Histoplasma capsulatum*. *J Leukoc Biol* 43: 483-491.
- 56
57 762 Fevre, C., Almeida, A.S., Taront, S., Pedron, T., Huerre, M., Prevost, M.C., *et al* (2013) A novel
58 763 murine model of rhinoscleroma identifies Mikulicz cells, the disease signature, as IL-10 dependent
59 764 derivatives of inflammatory monocytes. *EMBO Mol Med* 5: 516-530.
- 60
61 765 Fink, S.L., and Cookson, B.T. (2007) Pyroptosis and host cell death responses during *Salmonella*
62 766 infection. *Cell Microbiol* 9: 2562-2570.

- 1
2 767 Flannagan, R.S., Cosio, G., and Grinstein, S. (2009) Antimicrobial mechanisms of phagocytes and
3 768 bacterial evasion strategies. *Nat Rev Microbiol* 7: 355-366.
- 4 769 Flannagan, R.S., Jaumouille, V., and Grinstein, S. (2012) The cell biology of phagocytosis. *Annu*
5 770 *Rev Pathol* 7: 61-98.
- 7 771 Fortier, A.H., Leiby, D.A., Narayanan, R.B., Asafoadjei, E., Crawford, R.M., Nacy, C.A., *et al*
8 772 (1995) Growth of *Francisella tularensis* LVS in macrophages: the acidic intracellular compartment
9 773 provides essential iron required for growth. *Infect Immun* 63: 1478-1483.
- 11 774 Frank, C.G., Reguerio, V., Rother, M., Moranta, D., Maeurer, A.P., Garmendia, J., *et al* (2013)
12 775 *Klebsiella pneumoniae* targets an EGF receptor-dependent pathway to subvert inflammation. *Cell*
13 776 *Microbiol* 15: 1212-1233.
- 15 777 Garcia-del Portillo, F., Foster, J.W., Maguire, M.E., and Finlay, B.B. (1992) Characterization of the
16 778 micro-environment of *Salmonella typhimurium*-containing vacuoles within MDCK epithelial cells.
17 779 *Mol Microbiol* 6: 3289-3297.
- 18 780 Geier, H., and Celli, J. (2011) Phagocytic receptors dictate phagosomal escape and intracellular
19 781 proliferation of *Francisella tularensis*. *Infect Immun* 79: 2204-2214.
- 21 782 Ghigo, E., Capo, C., Aurouze, M., Tung, C.H., Gorvel, J.P., Raoult, D., *et al* (2002) Survival of
22 783 *Tropheryma whipplei*, the agent of Whipple's disease, requires phagosome acidification. *Infect*
23 784 *Immun* 70: 1501-1506.
- 25 785 Gordon, S.B., Irving, G.R., Lawson, R.A., Lee, M.E., and Read, R.C. (2000) Intracellular
26 786 trafficking and killing of *Streptococcus pneumoniae* by human alveolar macrophages are influenced
27 787 by opsonins. *Infect Immun* 68: 2286-2293.
- 29 788 Greco, E., Quintiliani, G., Santucci, M.B., Serafino, A., Ciccaglione, A.R., Marcantonio, C., *et al*
30 789 (2012) Janus-faced liposomes enhance antimicrobial innate immune response in *Mycobacterium*
31 790 *tuberculosis* infection. *Proc Natl Acad Sci U S A* 109: E1360-8.
- 33 791 Hilbi, H., Moss, J.E., Hersh, D., Chen, Y., Arondel, J., Banerjee, S., *et al* (1998) *Shigella*-induced
34 792 apoptosis is dependent on caspase-1 which binds to IpaB. *J Biol Chem* 273: 32895-32900.
- 35 793 Hmama, Z., Sendide, K., Talal, A., Garcia, R., Dobos, K., and Reiner, N.E. (2004) Quantitative
36 794 analysis of phagolysosome fusion in intact cells: inhibition by mycobacterial lipoarabinomannan
37 795 and rescue by an 1alpha,25-dihydroxyvitamin D3-phosphoinositide 3-kinase pathway. *J Cell Sci*
38 796 117: 2131-2140.
- 40 797 Hoogendijk, A.J., Diks, S.H., Peppelenbosch, M.P., Van Der Poll, T., and Wieland, C.W. (2011)
41 798 Kinase activity profiling of gram-negative pneumonia. *Mol Med* 17: 741-747.
- 43 799 Howe, D., and Mallavia, L.P. (2000) *Coxiella burnetii* exhibits morphological change and delays
44 800 phagolysosomal fusion after internalization by J774A.1 cells. *Infect Immun* 68: 3815-3821.
- 46 801 Insua, J.L., Llobet, E., Moranta, D., Perez-Gutierrez, C., Tomas, A., Garmendia, J., *et al* (2013)
47 802 Modelling *Klebsiella pneumoniae* pathogenesis by infecting the wax moth *Galleria mellonella*.
48 803 *Infect Immun*. 81: 3552-3565.
- 49 804 Jordens, I., Fernandez-Borja, M., Marsman, M., Dusseljee, S., Janssen, L., Calafat, J., *et al* (2001)
50 805 The Rab7 effector protein RILP controls lysosomal transport by inducing the recruitment of dynein-
51 806 dynactin motors. *Curr Biol* 11: 1680-1685.
- 53 807 Krachler, A.M., Woolery, A.R., and Orth, K. (2011) Manipulation of kinase signaling by bacterial
54 808 pathogens. *J Cell Biol* 195: 1083-1092.
- 56 809 Kruskal, B.A., Sastry, K., Warner, A.B., Mathieu, C.E., and Ezekowitz, R.A. (1992) Phagocytic
57 810 chimeric receptors require both transmembrane and cytoplasmic domains from the mannose
58 811 receptor. *J Exp Med* 176: 1673-1680.

- 1
2 812 Kuijl, C., Savage, N.D., Marsman, M., Tuin, A.W., Janssen, L., Egan, D.A., *et al* (2007)
3 813 Intracellular bacterial growth is controlled by a kinase network around PKB/AKT1. *Nature* 450:
4 814 725-730.
- 5
6 815 Kyei, G.B., Vergne, I., Chua, J., Roberts, E., Harris, J., Junutula, J.R., *et al* (2006) Rab14 is critical
7 816 for maintenance of *Mycobacterium tuberculosis* phagosome maturation arrest. *EMBO J* 25: 5250-
8 817 5259.
- 9
10 818 Lamothe, J., Huynh, K.K., Grinstein, S., and Valvano, M.A. (2007) Intracellular survival of
11 819 *Burkholderia cenocepacia* in macrophages is associated with a delay in the maturation of bacteria-
12 820 containing vacuoles. *Cell Microbiol* 9: 40-53.
- 13
14 821 Lawlor, M.S., Handley, S.A., and Miller, V.L. (2006) Comparison of the host responses to wild-
15 822 type and *cpsB* mutant *Klebsiella pneumoniae* infections. *Infect Immun* 74: 5402-5407.
- 16
17 823 Lawlor, M.S., Hsu, J., Rick, P.D., and Miller, V.L. (2005) Identification of *Klebsiella pneumoniae*
18 824 virulence determinants using an intranasal infection model. *Mol Microbiol* 58: 1054-1073.
- 19
20 825 Manz, W., Szewzyk, U., Ericsson, P., Amann, R., Schleifer, K.H., and Stenstrom, T.A. (1993) In
21 826 situ identification of bacteria in drinking water and adjoining biofilms by hybridization with 16S
22 827 and 23S rRNA-directed fluorescent oligonucleotide probes. *Appl Environ Microbiol* 59: 2293-2298.
- 23
24 828 March, C., Cano, V., Moranta, D., Llobet, E., Perez-Gutierrez, C., Tomas, J.M., *et al* (2013) Role of
25 829 bacterial surface structures on the interaction of *Klebsiella pneumoniae* with phagocytes. *PLoS One*
26 830 8: e56847.
- 27
28 831 Miller, W.G., Leveau, J.H., and Lindow, S.E. (2000) Improved *gfp* and *inaZ* broad-host-range
29 832 promoter-probe vectors. *Mol Plant Microbe Interact* 13: 1243-1250.
- 30
31 833 Moranta, D., Regueiro, V., March, C., Llobet, E., Margareto, J., Larrarte, E., *et al* (2010) *Klebsiella*
32 834 *pneumoniae* capsule polysaccharide impedes the expression of beta-defensins by airway epithelial
33 835 cells. *Infect Immun* 78: 1135-1146.
- 34
35 836 Morey, P., Cano, V., Marti-Llitas, P., Lopez-Gomez, A., Regueiro, V., Saus, C., *et al* (2011)
36 837 Evidence for a non-replicative intracellular stage of nontypable *Haemophilus influenzae* in
37 838 epithelial cells. *Microbiology* 157: 234-250.
- 38
39 839 Munoz-Price, L.S., Poirel, L., Bonomo, R.A., Schwaber, M.J., Daikos, G.L., Cormican, M., *et al*
40 840 (2013) Clinical epidemiology of the global expansion of *Klebsiella pneumoniae* carbapenemases.
41 841 *Lancet Infect Dis* 13: 785-796.
- 42
43 842 Navarre, W.W., and Zychlinsky, A. (2000) Pathogen-induced apoptosis of macrophages: a common
44 843 end for different pathogenic strategies. *Cell Microbiol* 2: 265-273.
- 45
46 844 Oelschlaeger, T.A., and Tall, B.D. (1997) Invasion of cultured human epithelial cells by *Klebsiella*
47 845 *pneumoniae* isolated from the urinary tract. *Infect Immun* 65: 2950-2958.
- 48
49 846 Porte, F., Liautard, J.P., and Kohler, S. (1999) Early acidification of phagosomes containing
50 847 *Brucella suis* is essential for intracellular survival in murine macrophages. *Infect Immun* 67: 4041-
51 848 4047.
- 52
53 849 Regueiro, V., Campos, M.A., Pons, J., Alberti, S., and Bengoechea, J.A. (2006) The uptake of a
54 850 *Klebsiella pneumoniae* capsule polysaccharide mutant triggers an inflammatory response by human
55 851 airway epithelial cells. *Microbiology* 152: 555-566.
- 56
57 852 Repetto, G., del Peso, A., and Zurita, J.L. (2008) Neutral red uptake assay for the estimation of cell
58 853 viability/cytotoxicity. *Nat Protoc* 3: 1125-1131.
- 59
60 854 Rink, J., Ghigo, E., Kalaidzidis, Y., and Zerial, M. (2005) Rab conversion as a mechanism of
855 progression from early to late endosomes. *Cell* 122: 735-749.

- 1
2 856 Sahly, H., and Podschun, R. (1997) Clinical, bacteriological, and serological aspects of *Klebsiella*
3 857 infections and their spondylarthropathic sequelae. *Clin Diagn Lab Immunol* 4: 393-399.
- 4
5 858 Sarantis, H., and Grinstein, S. (2012) Subversion of phagocytosis for pathogen survival. *Cell Host*
6 859 *Microbe* 12: 419-431.
- 7
8 860 Seto, S., Tsujimura, K., and Koide, Y. (2011) Rab GTPases regulating phagosome maturation are
9 861 differentially recruited to mycobacterial phagosomes. *Traffic* 12: 407-420.
- 10
11 862 Smith, A.C., Heo, W.D., Braun, V., Jiang, X., Macrae, C., Casanova, J.E., *et al* (2007) A network
12 863 of Rab GTPases controls phagosome maturation and is modulated by *Salmonella enterica* serovar
13 864 Typhimurium. *J Cell Biol* 176: 263-268.
- 14
15 865 Thi, E.P., and Reiner, N.E. (2012) Phosphatidylinositol 3-kinases and their roles in phagosome
16 866 maturation. *J Leukoc Biol* 92: 553-566.
- 17
18 867 Trombetta, E.S., and Mellman, I. (2005) Cell biology of antigen processing in vitro and in vivo.
19 868 *Annu Rev Immunol* 23: 975-1028.
- 20
21 869 Vieira, O.V., Botelho, R.J., and Grinstein, S. (2002) Phagosome maturation: aging gracefully.
22 870 *Biochem J* 366: 689-704.
- 23
24 871 Vieira, O.V., Botelho, R.J., Rameh, L., Brachmann, S.M., Matsuo, T., Davidson, H.W., *et al* (2001)
25 872 Distinct roles of class I and class III phosphatidylinositol 3-kinases in phagosome formation and
26 873 maturation. *J Cell Biol* 155: 19-25.
- 27
28 874 von Bargen, K., Gorvel, J.P., and Salcedo, S.P. (2012) Internal affairs: investigating the *Brucella*
29 875 intracellular lifestyle. *FEMS Microbiol Rev* 36: 533-562.
- 30
31 876 Willingham, S.B., Allen, I.C., Bergstralh, D.T., Brickey, W.J., Huang, M.T., Taxman, D.J., *et al*
32 877 (2009) NLRP3 (NALP3, Cryopyrin) facilitates in vivo caspase-1 activation, necrosis, and HMGB1
33 878 release via inflammasome-dependent and -independent pathways. *J Immunol* 183: 2008-2015.
- 34
35 879 Willingham, S.B., Bergstralh, D.T., O'Connor, W., Morrison, A.C., Taxman, D.J., Duncan, J.A., *et*
36 880 *al* (2007) Microbial pathogen-induced necrotic cell death mediated by the inflammasome
37 881 components CIAS1/cryopyrin/NLRP3 and ASC. *Cell Host Microbe* 2: 147-159.
- 38
39 882 Wu, J., Kobayashi, M., Sousa, E.A., Liu, W., Cai, J., Goldman, S.J., *et al* (2005) Differential
40 883 proteomic analysis of bronchoalveolar lavage fluid in asthmatics following segmental antigen
41 884 challenge. *Mol Cell Proteomics* 4: 1251-1264.
- 42
43 885 Yu, X.J., McGourty, K., Liu, M., Unsworth, K.E., and Holden, D.W. (2010) pH sensing by
44 886 intracellular *Salmonella* induces effector translocation. *Science* 328: 1040-1043.
- 45
46 887 Zimmerli, S., Edwards, S., and Ernst, J.D. (1996) Selective receptor blockade during phagocytosis
47 888 does not alter the survival and growth of *Mycobacterium tuberculosis* in human macrophages. *Am J*
48 889 *Respir Cell Mol Biol* 15: 760-770.

890

891

1
2
3
4
5
6
7
8
9
10
11
12
13
14
15
16
17
18
19
20
21
22
23
24
25
26
27
28
29
30
31
32
33
34
35
36
37
38
39
40
41
42
43
44
45
46
47
48
49
50
51
52
53
54
55
56
57
58
59
60

892 **FIGURE LEGENDS**

893 **FIGURE 1. Phagocytosis of *K. pneumoniae* by macrophages.**

894 (A) Immunofluorescence confocal microscopy showing the lack of colocalisation between *K.*
895 *pneumoniae* and the lysosome marker cathepsin D in macrophages isolated from the BALF of
896 infected mice with *K. pneumoniae* harbouring pFPV25.1Cm. Methanol fixation was used for
897 cathepsin D staining. (B) Involvement of PI3K, cytoskeleton and lipid rafts on Kp43816R
898 phagocytosis by MH-S cells. (C) Immunoblot analysis of Akt phosphorylation (P-Akt) in lysates of
899 MH-S cells infected with Kp43816R for the indicated times. Membranes were probed for tubulin as
900 a loading control. Data are representative of three independent experiments. (D) Immunoblot
901 analysis of Akt phosphorylation (P-Akt) in lysates of PI3K inhibitor (LY294002) or DMSO
902 (vehicle solution)-treated MH-S cells infected with Kp43816R for 20 min. Membranes were probed
903 for tubulin as a loading control. Data are representative of three independent experiments. (E) TEM
904 analysis of MH-S macrophages infected with Kp43816R for the indicated time points. Data are
905 representative of two independent experiments. (F) Detection of FISH positive Kp43816R inside
906 MH-S cells 5.5 h post infection. Kp43816R harbored pFPV25.1Cm (green), host cell nuclei were
907 stained with Hoechst (blue), and metabolically active bacteria were labelled with probes EUB338-
908 Cy3 and GAM42a-Cy3 (red). (G) Quantification of the number of metabolically active (FISH
909 positive) intracellular bacteria in MH-S infected cells. Results are represented as percentage of
910 FISH positive bacteria versus total number of intracellular bacteria (green). At least 300 infected
911 cells belonging to three independent experiments were counted per time point.

912 **FIGURE 2. Dynamics of *K. pneumoniae* survival in macrophages.**

913 (A) MH-S cells were infected with Kp43816R for 30 min (MOI 50:1). Wells were washed and
914 incubated with medium containing gentamicin (300 µg/ml) and polymyxin B (15 µg/ml) for 90 min
915 to eliminate extracellular bacteria, and then with medium containing gentamicin 100 µg/ml for up to
916 12.5 h. Intracellular bacteria were quantified by lysis, serial dilution and viable counting on LB agar
917 plates. (B) MH-S cells were infected with Kp43816R harboring pFPV25.1Cm and the phagocytic

1
2 918 index calculated as the number of intracellular bacteria (determined by extra-/intracellular
3
4 919 differential staining) per the percentage of infected cells. (C) Quantification of intracellular bacteria
5
6 920 in mTHP-1 cells infected with Kp43816R. (D) Phagocytic index of infected mTHP-1 cells.

7
8 921 In panels A and C, data, shown as $\text{Log}_{10}\text{CFU/well}$, are the average of three independent
9
10 922 experiments. In panels B and D, at least 500 infected cells belonging to three independent
11
12 923 experiments were counted per time point.

13
14
15 924 **FIGURE 3. Apoptosis of MH-S cells.**

16
17 925 (A) MH-S cells were mock-treated or infected with Kp43816R harboring pFPV25.1Cm. 6 h post
18
19 926 infection, cells were stained with Annexin V and 7-AAD and analysed by flow cytometry. A
20
21 927 representative experiment of three is shown. (B) Data from three independent experiments are
22
23 928 represented as mean \pm SD.

24
25
26 929 **FIGURE 4. Phagosome maturation during *K. pneumoniae* infection of MH-S cells.**

27
28 930 (A) Upper and middle panels show the colocalization of Kp43816R harboring pFPV25.1Cm and
29
30 931 EEA1 (images were taken 30 min post infection) and Lamp1 (images were taken 4 h post
31
32 932 infection) using goat anti-EEA1 and donkey anti-goat conjugated to Rhodamine, and rat anti-Lamp-
33
34 933 1 and donkey anti-rat conjugated to Rhodamine antibodies, respectively. Lower panels show the
35
36 934 colocalization of Kp43816R and EGFP-Rab7 and RILP-C33-EGFP (images were taken 4 h post
37
38 935 infection). Bacteria were stained using rabbit anti-*Klebsiella* and donkey anti-rabbit conjugated to
39
40 936 Rhodamine antibodies. Images are representative of triplicate coverslips in three independent
41
42 937 experiments.

43
44
45 938 (B) Percentage of Kp43816R colocalization with EEA1, Lamp1, and EGFP-Rab7 and RILP-C33-
46
47 939 EGFP over a time course. Cells were infected, coverslips were fixed and stained at the indicated
48
49 940 times. Values are given as mean percentage of Kp43816R colocalizing with the marker \pm SE. At
50
51 941 least 300 infected cells belonging to three independent experiments were counted per time point.

52
53
54 942 **FIGURE 5. Colocalization of *K. pneumoniae* with phagolysosomal markers.**

1
2 943 (A) Upper panels show the colocalization of Kp43816R harboring pFPV25.1Cm and the dye
3
4 944 LysoTracker at 4 h post infection. Middle panels show the colocalization of Kp43816R harboring
5
6 945 pFPV25.1Cm and cathepsin D at 2 h post infection. Cathepsin D was stained using goat anti-human
7
8 946 cathepsin D (G19) and donkey anti-goat conjugated to Rhodamine antibodies. Lower panels display
9
10 947 the colocalization of Kp43816R harboring pFPV25.1Cm and TR-dextran at 2 h post infection.
11
12 948 Images are representative of three independent experiments. (B) Percentage of Kp43816R
13
14 949 colocalization with LysoTracker, cathepsin D and TR-dextran over a time course. Cells were
15
16 950 infected, coverslips were fixed and stained at the indicated times. Values are given as mean
17
18 951 percentage of Kp43816R colocalizing with the marker \pm SE. At least 300 infected cells belonging
19
20 952 to three independent experiments were counted per time point.
21
22

23
24 953 **FIGURE 6. Effect of vacuolar acidification on *K. pneumoniae* survival.**

25
26 954 (A) Microscopy analysis showing that bafilomycin A₁ (100 nM) treatment abrogates LysoTracker
27
28 955 staining of the KCV (images were taken at 4 h post infection). MH-S cells were infected with
29
30 956 Kp43816R harboring pFPV25.1Cm. Images are representative of triplicate coverslips in two
31
32 957 independent experiments. (B) Experimental outline to investigate the effect of vacuolar acidification
33
34 958 on the intracellular survival of Kp43816R. (C) Intracellular bacteria in MH-S cells, treated (white
35
36 959 symbols) or not (black symbols) with bafilomycin A₁, were quantified by lysis, serial dilution and
37
38 960 viable counting on LB agar plates. Data, shown as CFU/well, are the average of three independent
39
40 961 experiments. Significance testing performed by Log Rank test. *, $P < 0.05$.
41
42

43
44 962 **FIGURE 7. PI3K-AKT and Rab14 aid intracellular survival of *K. pneumoniae*.**

45
46 963 (A) Quantification of intracellular bacteria in MH-S cells infected with Kp43816R which were
47
48 964 mock-treated (black bar) or treated with LY294002 hydrochloride (75 μ M) or with AKT X (10
49
50 965 μ M). Treatments were added after the time of contact and kept until cells were lysed for bacterial
51
52 966 enumeration. Data, shown as CFU/well, are the average of three independent experiments. *, $P <$
53
54 967 0.05 (results are significantly different from the results for untreated cells; Mann-Whitney U test).
55
56 968 (B) Percentage of Kp43816R colocalization with TR-dextran in cells mock-treated or treated with
57
58
59
60

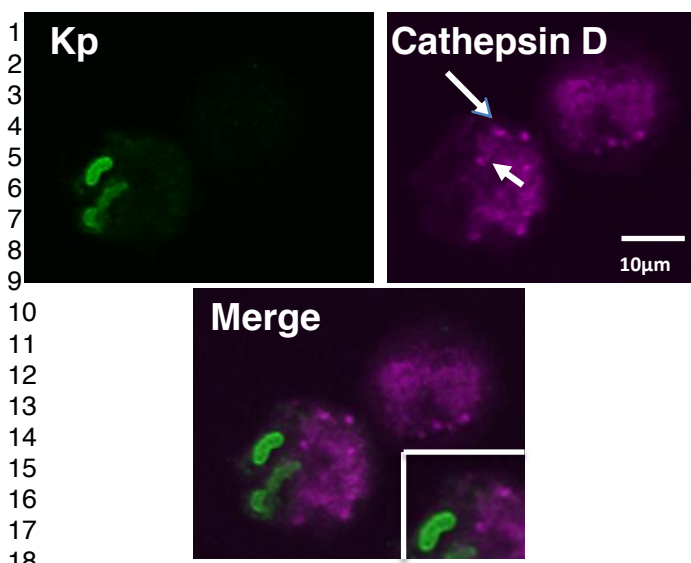
1 969 the Akt inhibitor AKT X over a time course. Cells were infected, coverslips were fixed and stained
2
3
4 970 at the indicated times. Treatments were added after the time of contact and kept until cells were
5
6 971 fixed. Values are given as mean percentage of Kp43816R colocalizing with the marker \pm SE. At
7
8 972 least 300 infected cells belonging to three independent experiments were counted per time point. *,
9
10 973 $P < 0.05$ (results are significantly different from the results for untreated cells; Mann-Whitney U
11
12 974 test). (C) Colocalization of Kp43816 and EGFP-Rab14 (image was taken 3.5 h post infection) in
13
14 975 MH-S cells. Bacteria were stained using rabbit anti-*Klebsiella* and donkey anti-rabbit conjugated to
15
16 976 Rhodamine antibodies. Image is representative of three independent experiments. Left graph shows
17
18 977 the percentage of Kp43816R colocalization with EGFP-Rab14 over a time course. Cells were
19
20 978 infected, coverslips were fixed and stained at the indicated times. Values are given as mean
21
22 979 percentage of Kp43816R colocalizing with the marker \pm SE. At least 300 infected cells belonging
23
24 980 to three independent experiments were counted per time point. (D) Quantification of intracellular
25
26 981 bacteria in transfected MH-S cells with plasmid pcDNA3 or with Rab14 dominant-negative
27
28 982 construct (DN-Rab14) at 3.5 h post infection. Data, shown as CFU/well, are the average of three
29
30 983 independent experiments. *, $P < 0.05$ (results are significantly different from the results for cells
31
32 984 transfected with control plasmid pcDNA3; Mann-Whitney U test).

33
34
35
36
37 985 **FIGURE 8. Role of CPS in *K. pneumoniae* intracellular survival.**

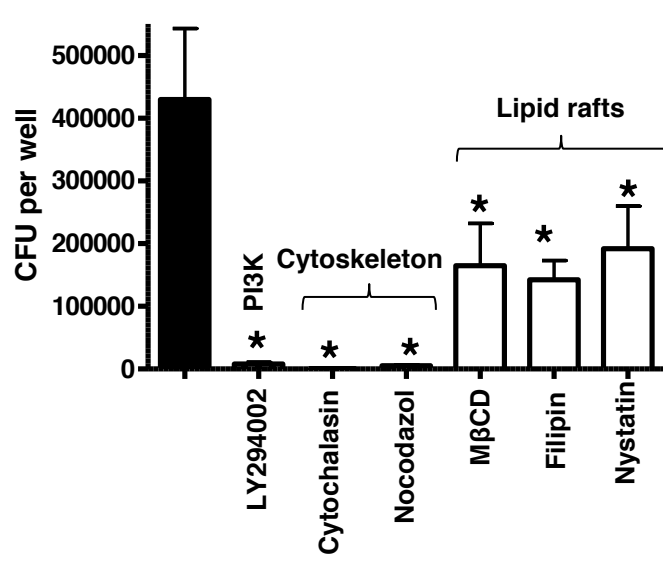
38
39 986 (A) MH-S or mTHP-1 cells were infected with Kp43816R (black symbols) or the capsule mutant
40
41 987 (Kp43816des; white symbols) for 30 min. Wells were washed and incubated with medium
42
43 988 containing gentamicin (300 μ g/ml) and polymyxin B (15 μ g/ml) for 90 min to eliminate
44
45 989 extracellular bacteria, and then with medium containing gentamicin 100 μ g/ml for up to 10 h.
46
47 990 Intracellular bacteria were quantified by lysis, serial dilution and viable counting on LB agar plates.
48
49 991 Data, shown as Log₁₀CFU/well, are the average of three independent experiments. (B) Opsonization
50
51 992 with 1% normal human sera (NHS) increased the phagocytosis of the capsule mutant
52
53 993 (Kp43816Rdes) by mTHP-1 cells. Data, shown as CFU/well, are the average of three independent
54
55 994 experiments. *, $P < 0.05$ (results are significantly different from the results for cells infected with
56
57
58
59
60

1
2 995 the non-opsionized capsule mutant; Mann-Whitney U test); n.s., no significant difference. (C)
3
4 996 mTHP-1 cells were infected for 30 min with Kp43816R or the capsule mutant which were either
5
6 997 opsonized or not. Wells were washed and incubated with medium containing gentamicin (300
7
8 998 $\mu\text{g/ml}$) and polymyxin B (15 $\mu\text{g/ml}$) for 90 min to eliminate extracellular bacteria, and then with
9
10 999 medium containing gentamicin 100 $\mu\text{g/ml}$ for up to 7.5 h. Intracellular bacteria were quantified by
11
12 1000 lysis, serial dilution and viable counting on LB agar plates. Data, shown as $\text{Log}_{10}\text{CFU/well}$, are the
13
14 1001 average of three independent experiments. Significance testing performed by Log Rank test. *, $P <$
15
16 1002 0.05. (D) Analysis of *cps::gfp* expression over time by flow cytometry. Analysis was performed
17
18 1003 after lysing MH-S cells and staining the bacteria using rabbit anti-*Klebsiella* and donkey anti-rabbit
19
20 1004 conjugated to Rhodamine antibodies (red histogram). In these populations, GFP fluorescence was
21
22 1005 analyzed (green histogram). Gray histogram represents GFP fluorescence for the negative-control
23
24 1006 sample, and the area of the histogram is considered negative for GFP fluorescence. Results are
25
26 1007 representative of three independent experiments. (E) Fluorescence levels of Kp43816R containing
27
28 1008 pPROBE'43Procps. Data, shown as relative fluorescence units (RFUs), are the average of three
29
30 1009 independent experiments. *, $P < 0.05$ (results are significantly different from the results for cells
31
32 1010 grown in medium buffered to pH 7.5; Mann-Whitney U test).
33
34
35
36
37
38
39
40
41
42
43
44
45
46
47
48
49
50
51
52
53
54
55
56
57
58
59
60

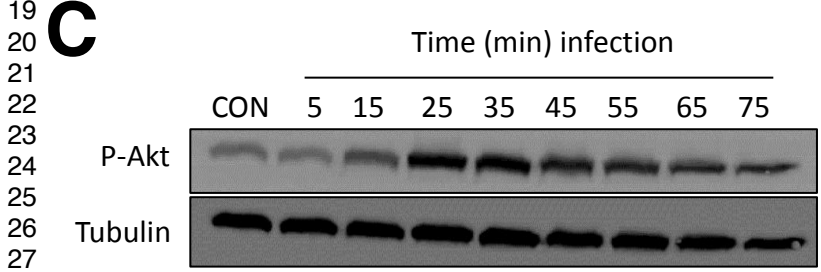
A



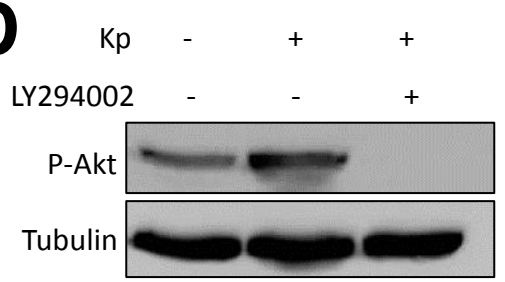
B



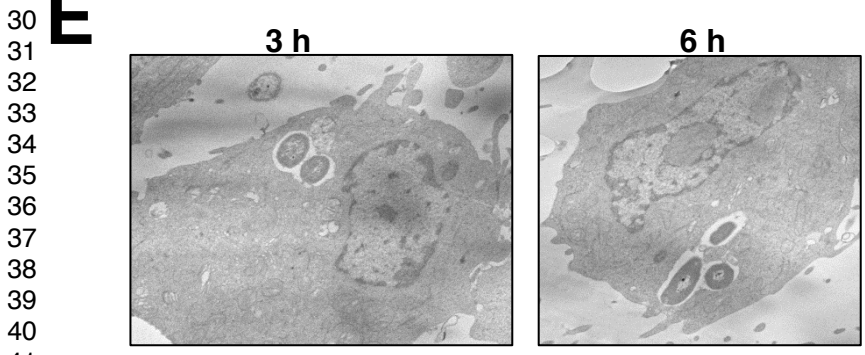
C



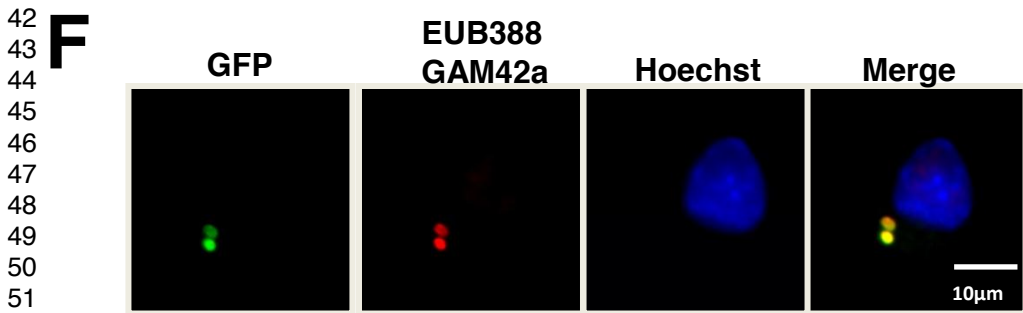
D



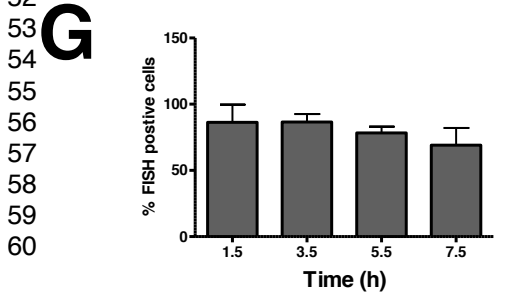
E

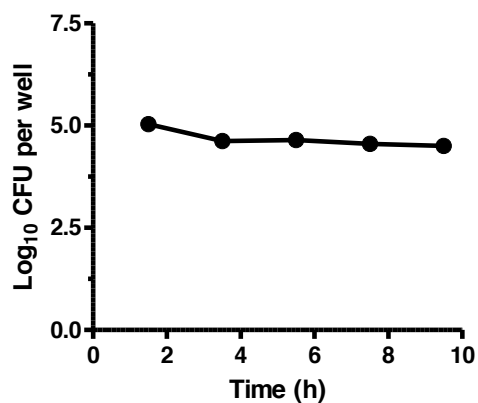
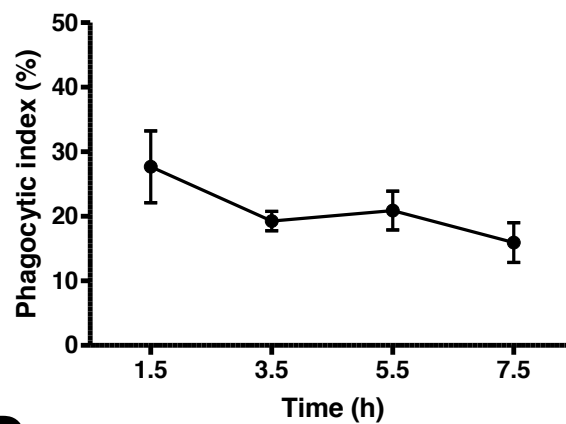
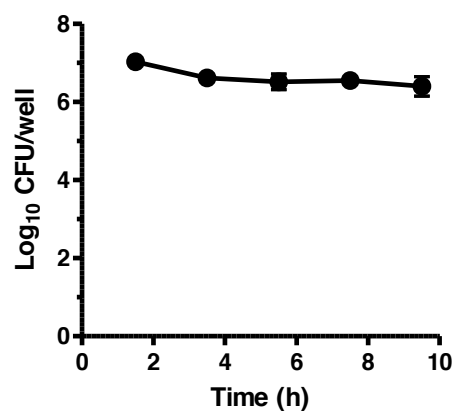
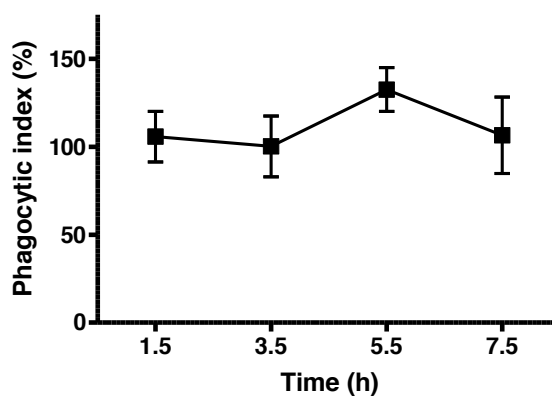


F



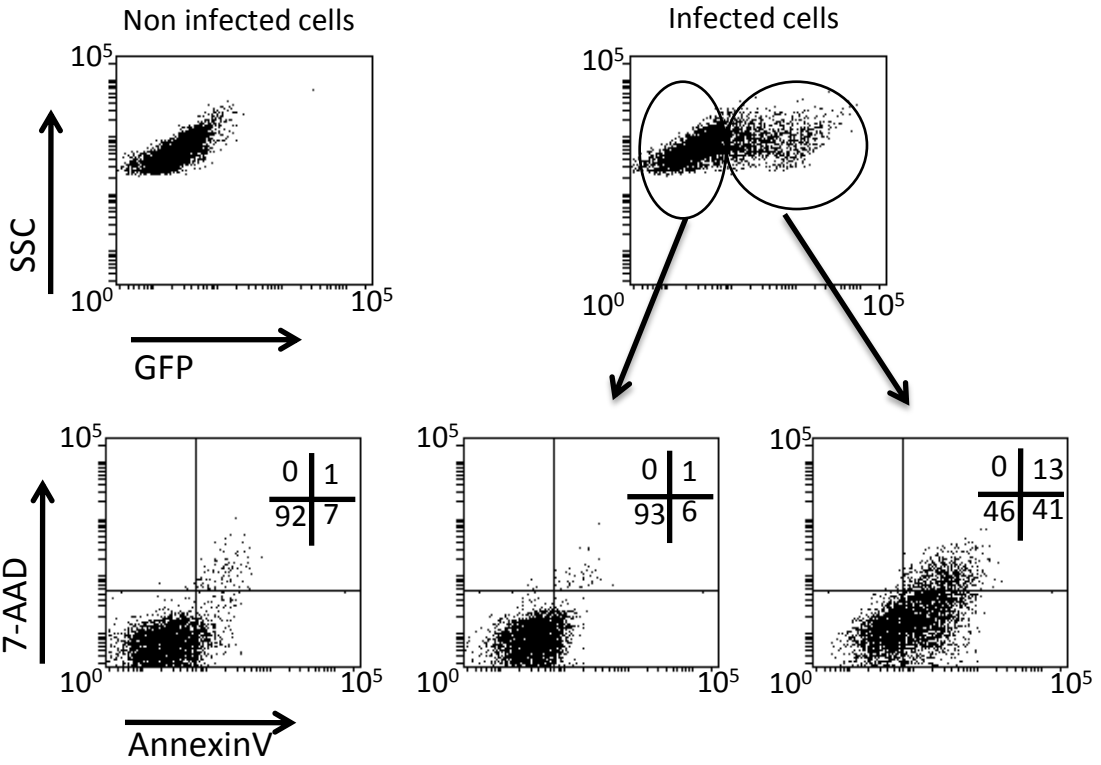
G



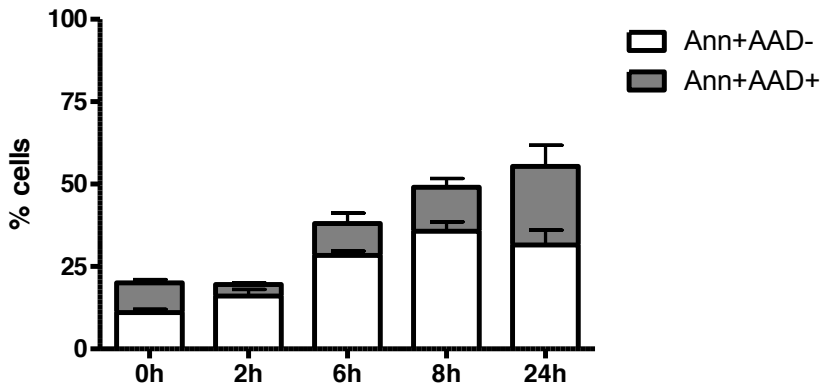
A**B****C****D**1
2
3
4
5
6
7
8
9
10
11
12
13
14
15
16
17
18
19
20
21
22
23
24
25
26
27
28
29
30
31
32
33
34
35
36
37
38
39
40
41
42
43
44
45
46
47
48
49
50
51
52
53
54
55
56
57
58
59
60

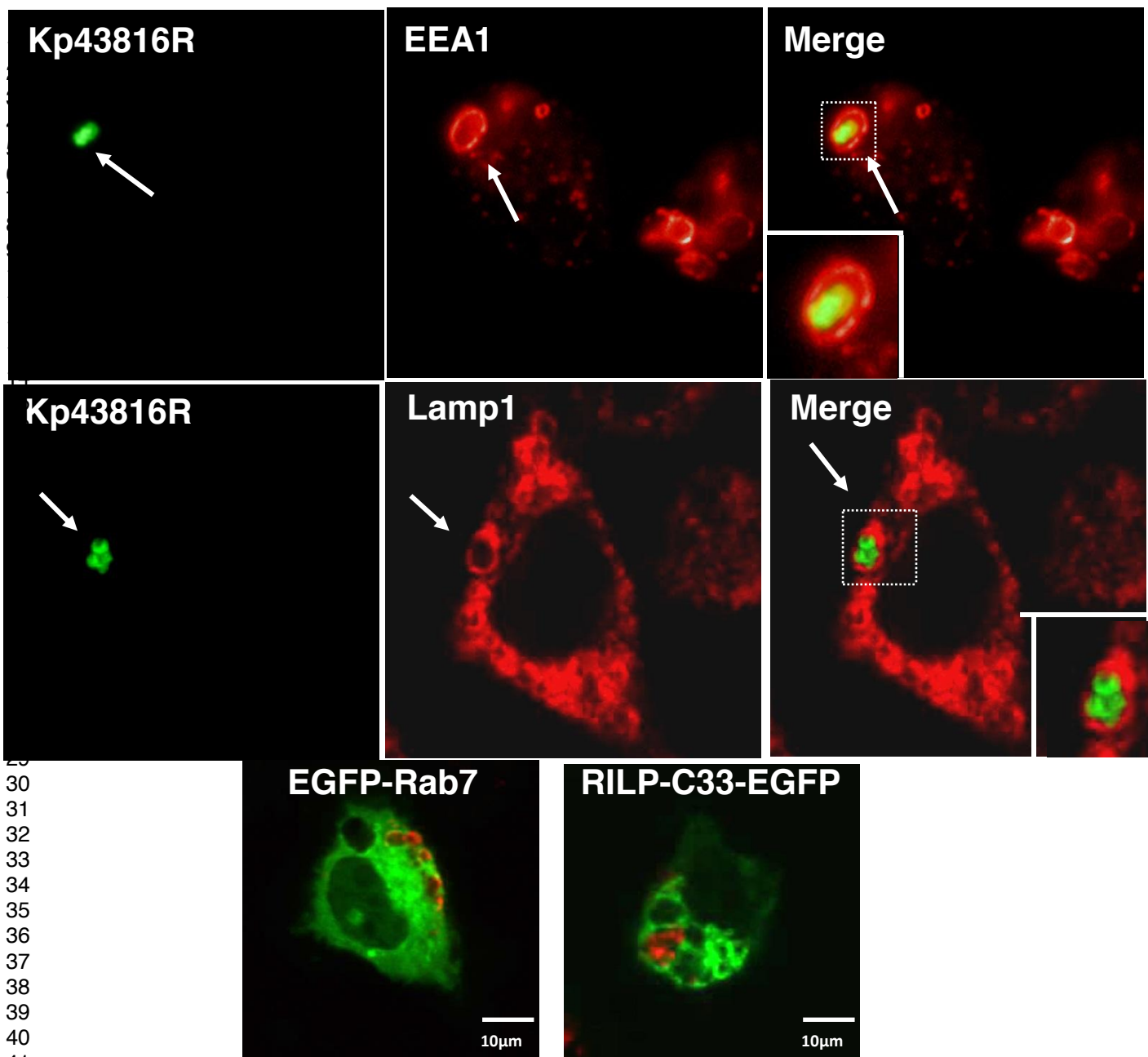
1
2
3
4
5
6
7
8
9
10
11
12
13
14
15
16
17
18
19
20
21
22
23
24
25
26
27
28
29
30
31
32
33
34
35
36
37
38
39
40
41
42
43
44
45
46
47
48
49
50
51
52
53
54
55
56
57
58
59
60

A

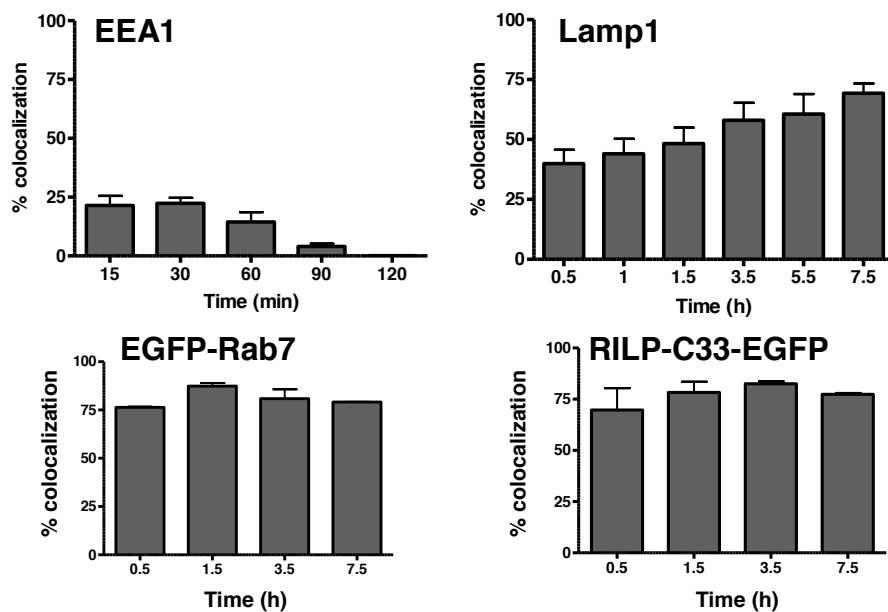


B

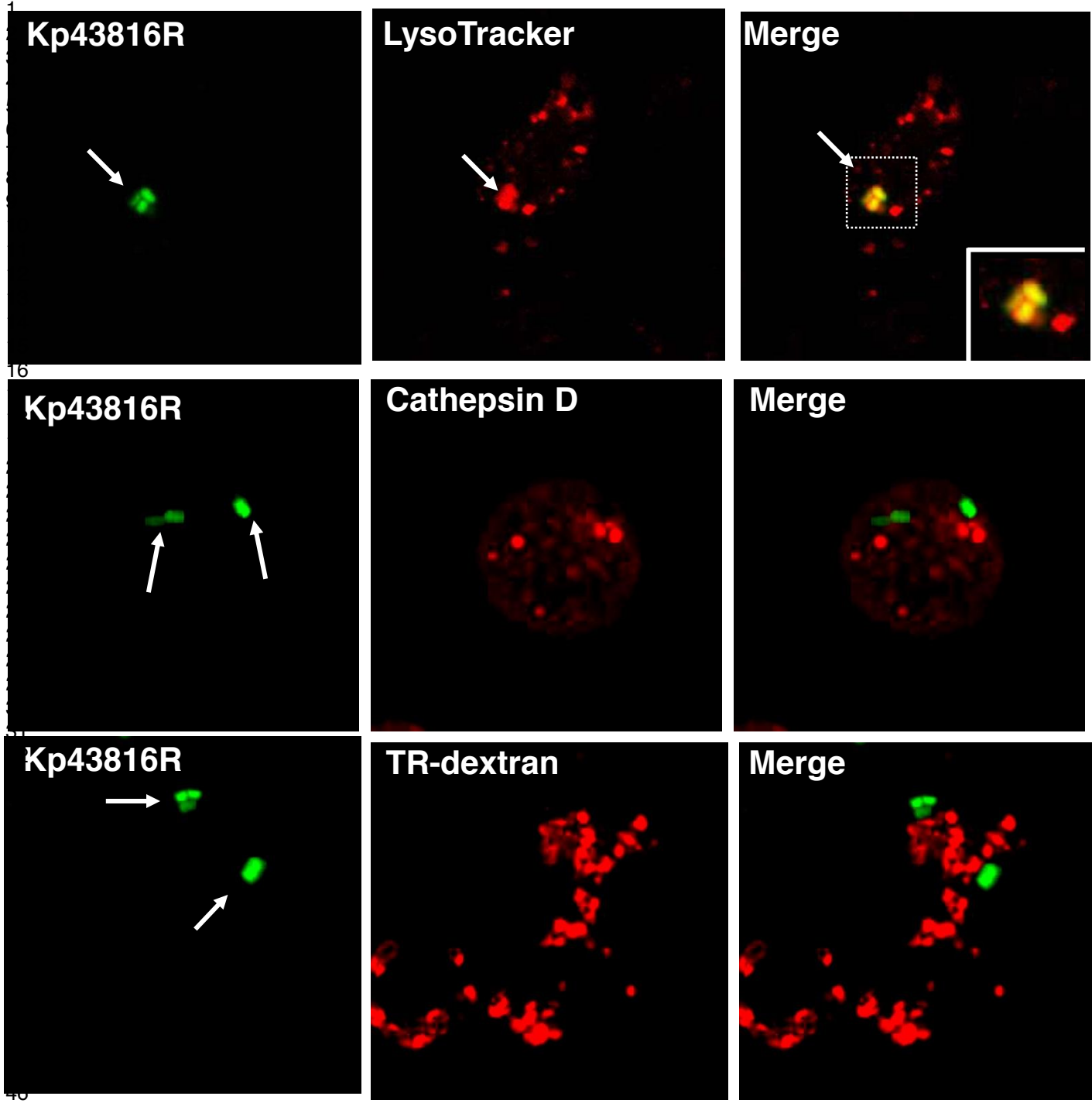




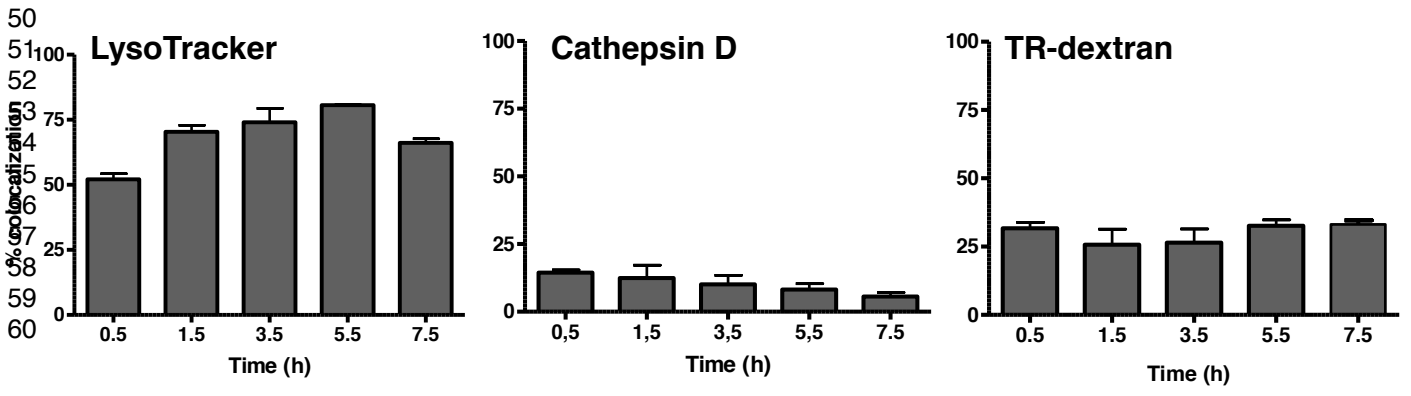
B



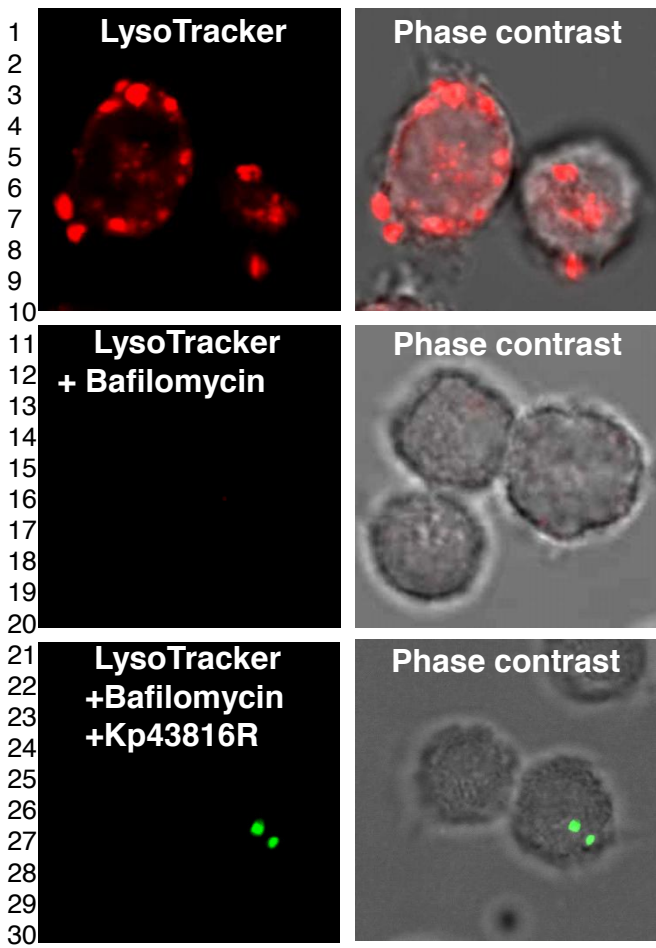
A



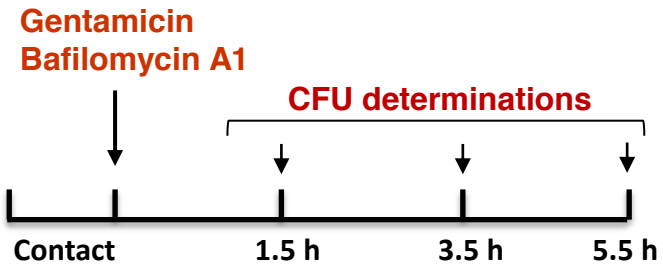
B



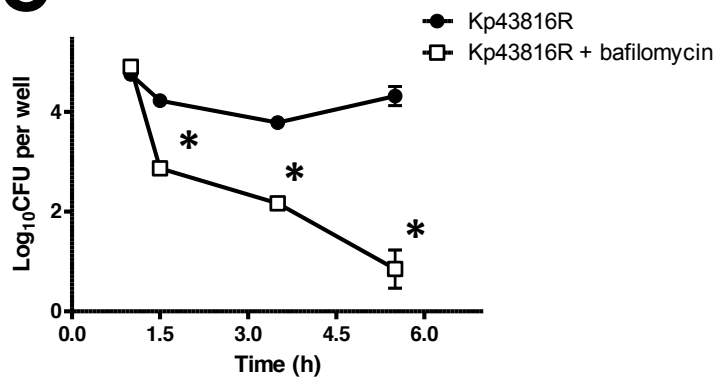
A

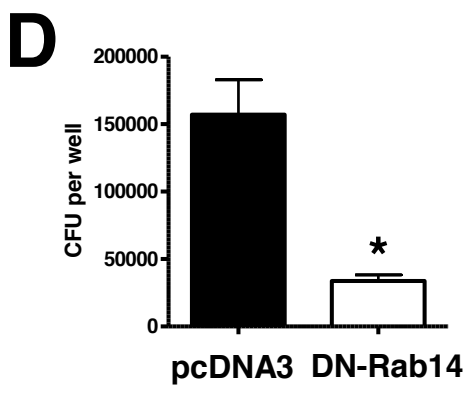
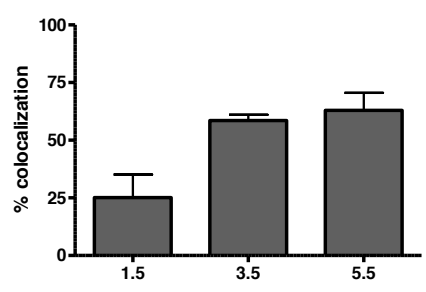
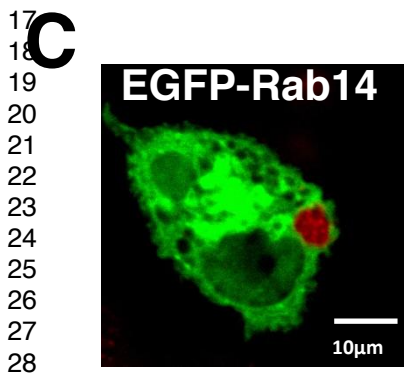
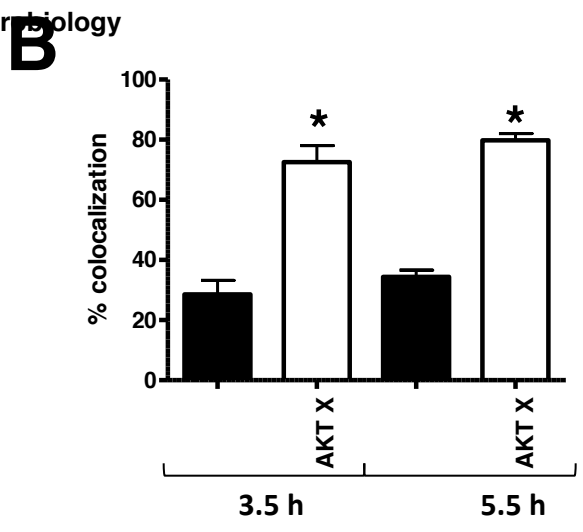
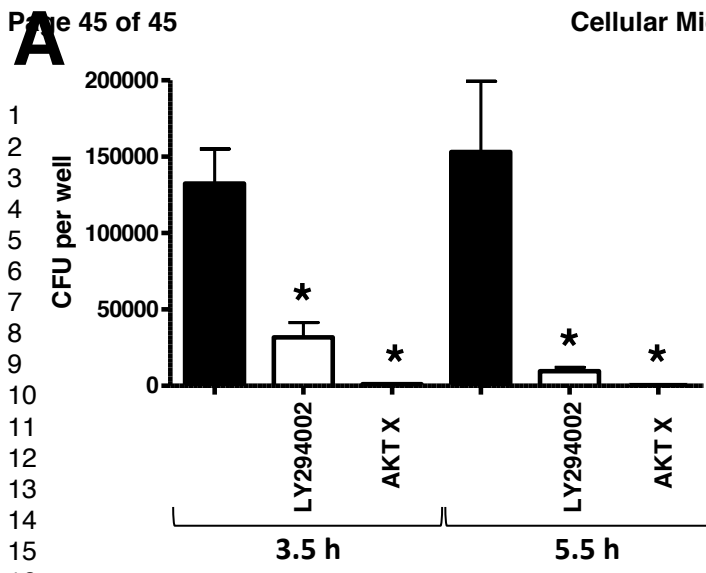


B



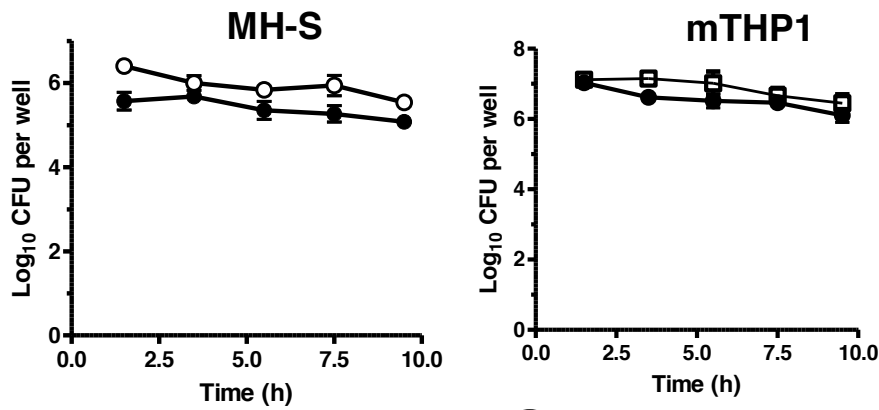
C



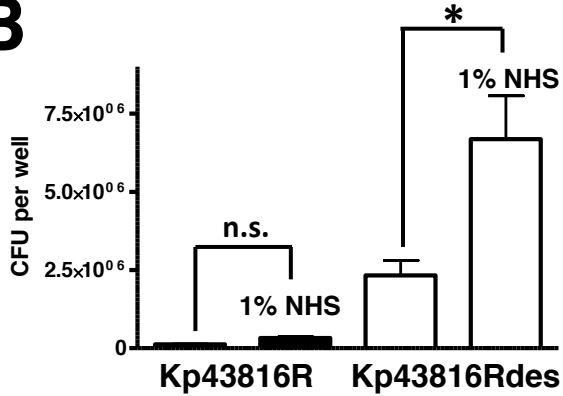


1
2
3
4
5
6
7
8
9
10
11
12
13
14
15
16
17
18
19
20
21
22
23
24
25
26
27
28
29
30
31
32
33
34
35
36
37
38
39
40
41
42
43
44
45
46
47
48
49
50
51
52
53
54
55
56
57
58
59
60

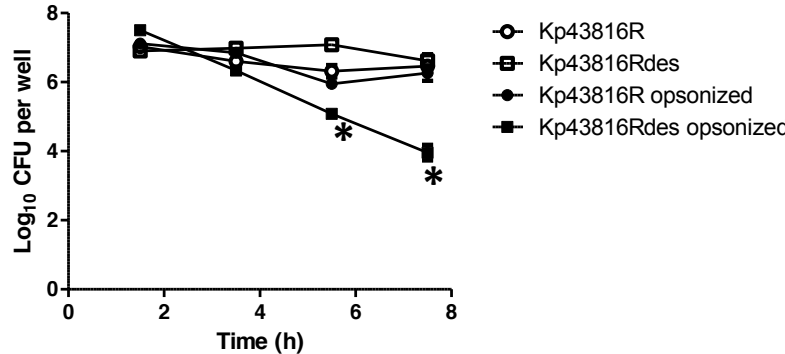
A



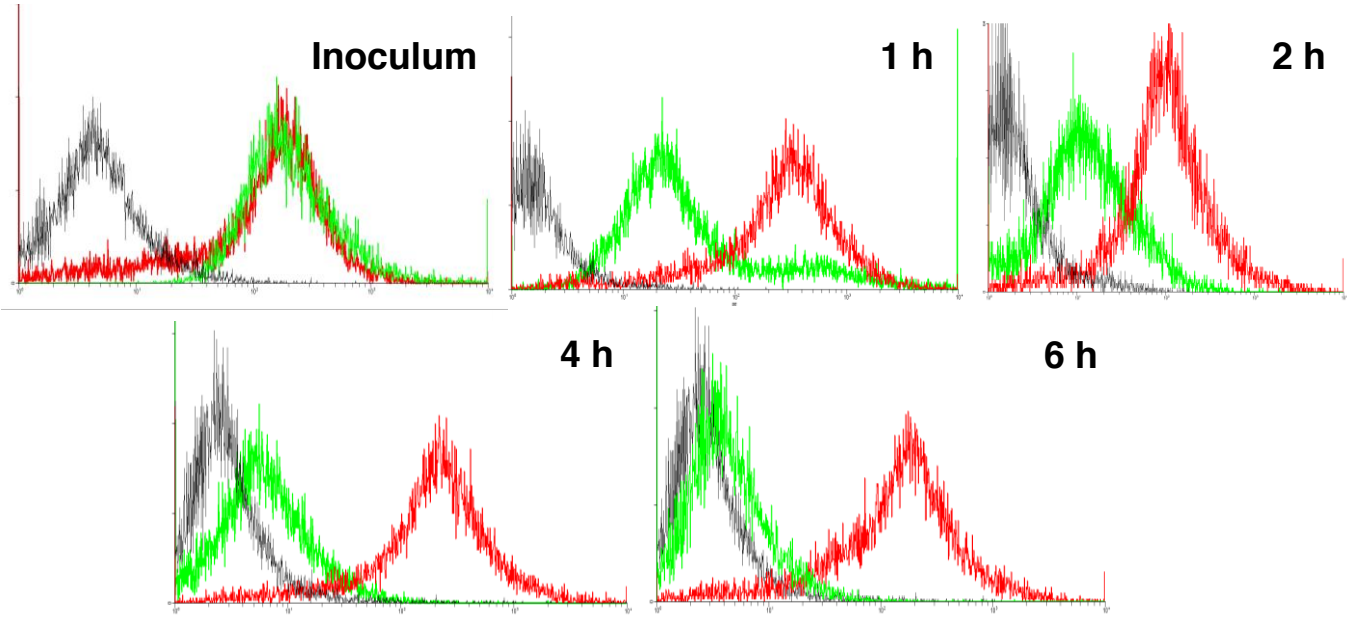
B



C



D



E

